

# Image Cover Sheet

**CLASSIFICATION**

UNCLASSIFIED

**SYSTEM NUMBER**

128263



**TITLE**

SOFTWARE DEVELOPMENT AND ANALYSIS FOR EXPERIMENTAL HIGH FREQUENCY  
SURFACE WAVE RADAR DATA

**System Number:**

**Patron Number:**

**Requester:**

**Notes:**

**DSIS Use only:**

**Deliver to:** JR





National  
Defence

Défense  
nationale



# SOFTWARE DEVELOPMENT AND ANALYSIS FOR EXPERIMENTAL HIGH FREQUENCY SURFACE WAVE RADAR DATA

by

**H.C. Chan**

**DEFENCE RESEARCH ESTABLISHMENT OTTAWA**  
REPORT NO. 1153

Canada

December 1992  
Ottawa



National  
Defence

Défense  
nationale

**SOFTWARE DEVELOPMENT AND ANALYSIS  
FOR EXPERIMENTAL HIGH FREQUENCY  
SURFACE WAVE RADAR DATA**

by

**H.C. Chan**  
*Surface Radar Section*  
*Radar Division*

**DEFENCE RESEARCH ESTABLISHMENT OTTAWA**  
REPORT NO. 1153

PCN  
041LR

December 1992  
Ottawa

^

^

^

^

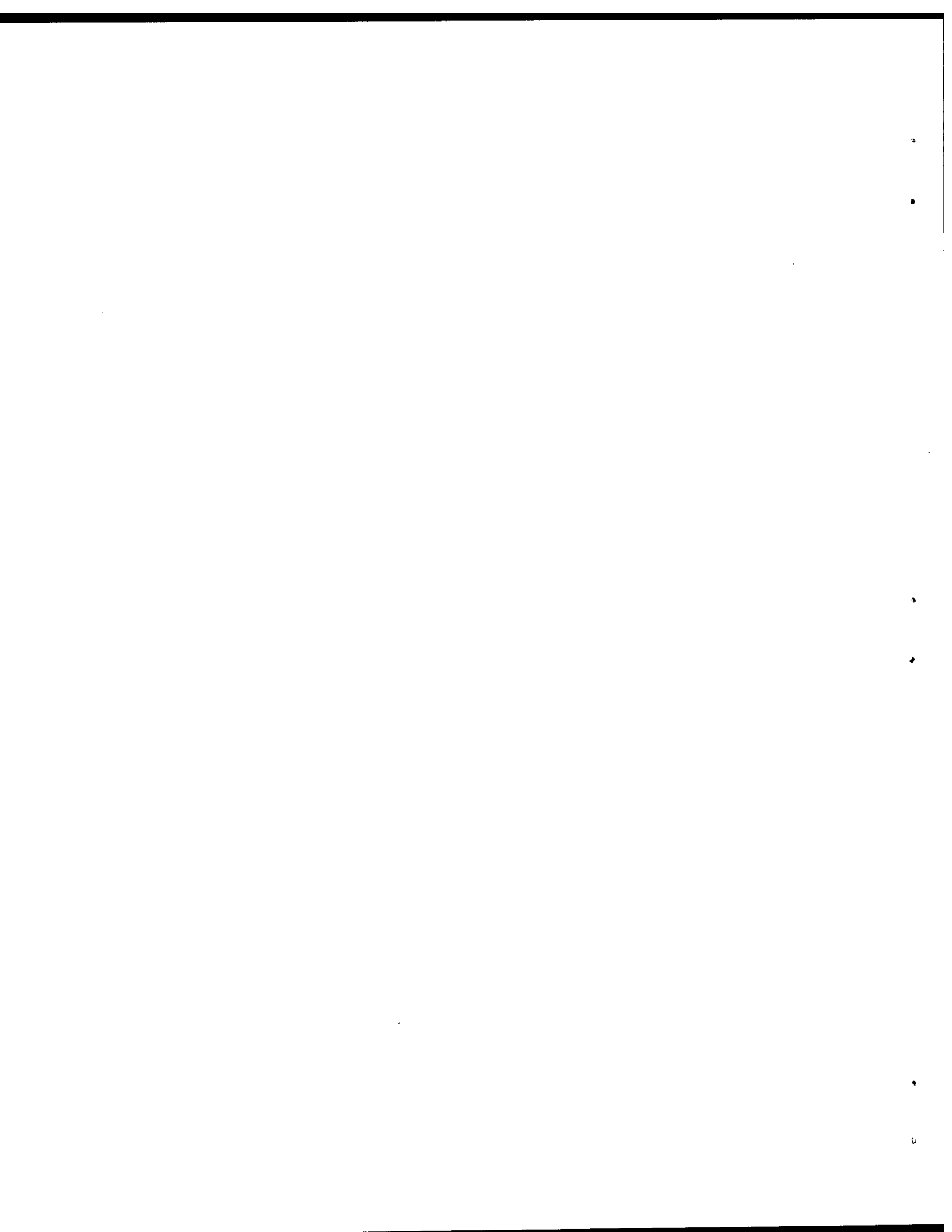
A

^

SOFTWARE DEVELOPMENT AND ANALYSIS FOR  
EXPERIMENTAL HIGH FREQUENCY SURFACE WAVE RADAR DATA

ABSTRACT

Processing software for data collected in an experimental High Frequency Surface Wave Radar (HFSWR) project is implemented in the VAX-3800 computer and the FPS-5000 floating point array processor. The software is used to process the data in-house so as to obtain insights in HFSWR sea clutter, noise and target characteristics. The data are examined to assess quality. Several deficiencies are observed in the data, including 60 Hz power source harmonic interferences and discontinuities in data sequences. Preliminary analysis of some of the data shows that conventional Doppler processing of the data permits the detection of ship and large aircraft targets at fairly long ranges. Plans for further analysis of these data are discussed.



# DÉVELOPPEMENT D'UN LOGICIEL ET ANALYSE DE DONNÉES POUR UN RADAR EXPÉRIMENTAL TRANSHORIZON À ONDES DÉCAMÉTRIQUES

## Résumé

Un logiciel pour le traitement des données recueillies par un radar expérimental transhorizon à ondes décimétriques a été développé sur un ordinateur VAX-3800 et un processeur vectoriel FPS-5000. Ce logiciel est utilisé pour traiter les données en laboratoire afin d'obtenir un aperçu des caractéristiques du fouillis de mer, du bruit et des cibles observées par le radar transhorizon à ondes décimétriques. Les données ont été examinées pour une analyse de la qualité. Plusieurs déficiences ont été observées dans les données, dont des interférences harmoniques de 60 Hz causées par l'alimentation électrique et des discontinuités dans les séquences de données. Une analyse préliminaire d'une partie des données a montré qu'un traitement Doppler conventionnel permet la détection de navires et de gros avions à de très grandes distances. Des plans pour des analyses plus détaillées de ces données sont présentés.



## EXECUTIVE SUMMARY

As an integral part of DREO's research in High Frequency Surface Wave Radar (HFSWR), data were collected by NORDCO Limited of Newfoundland under contract to DND, with the support of DREO and the Canadian Forces (CF). The Canadian Forces Auxiliary Vessel (CFAV) Bluethroat and an Aurora long range patrol aircraft were provided by the CF as test targets. A substantial amount of data were collected.

NORDCO Limited, which was the contractor responsible for analyzing and reporting on the data, was placed on receivership. As a result, the data tapes were brought back to DREO/RADAR for further analysis. The raw data required some pre-processing before detailed analysis could be done. The purpose of the work reported here was to develop the necessary software to analyze these data, to gain some insight into the characteristics of HF sea clutter and noise, and to assess the detection performance of HFSWR against various types of targets. This report documents the development of in-house pre-processing software and the findings during preliminary examination of these data.

The software was implemented in the VAX-3800 computer and the FPS-5000 floating point array processor. The data were examined to assess quality. Several deficiencies were observed in the data, including 60 Hz power source harmonic interferences and discontinuities in data sequences. Preliminary analysis of some of the data showed that conventional Doppler processing of the data permits the detection of ship and large aircraft targets at fairly long ranges. Plans for further analysis included spectral processing of the data (a) to determine the feasibility of employing HFSWR for medium range aircraft detection and long range ship detection, and (b) to investigate the characteristics of the direct over-head ionospheric reflection.

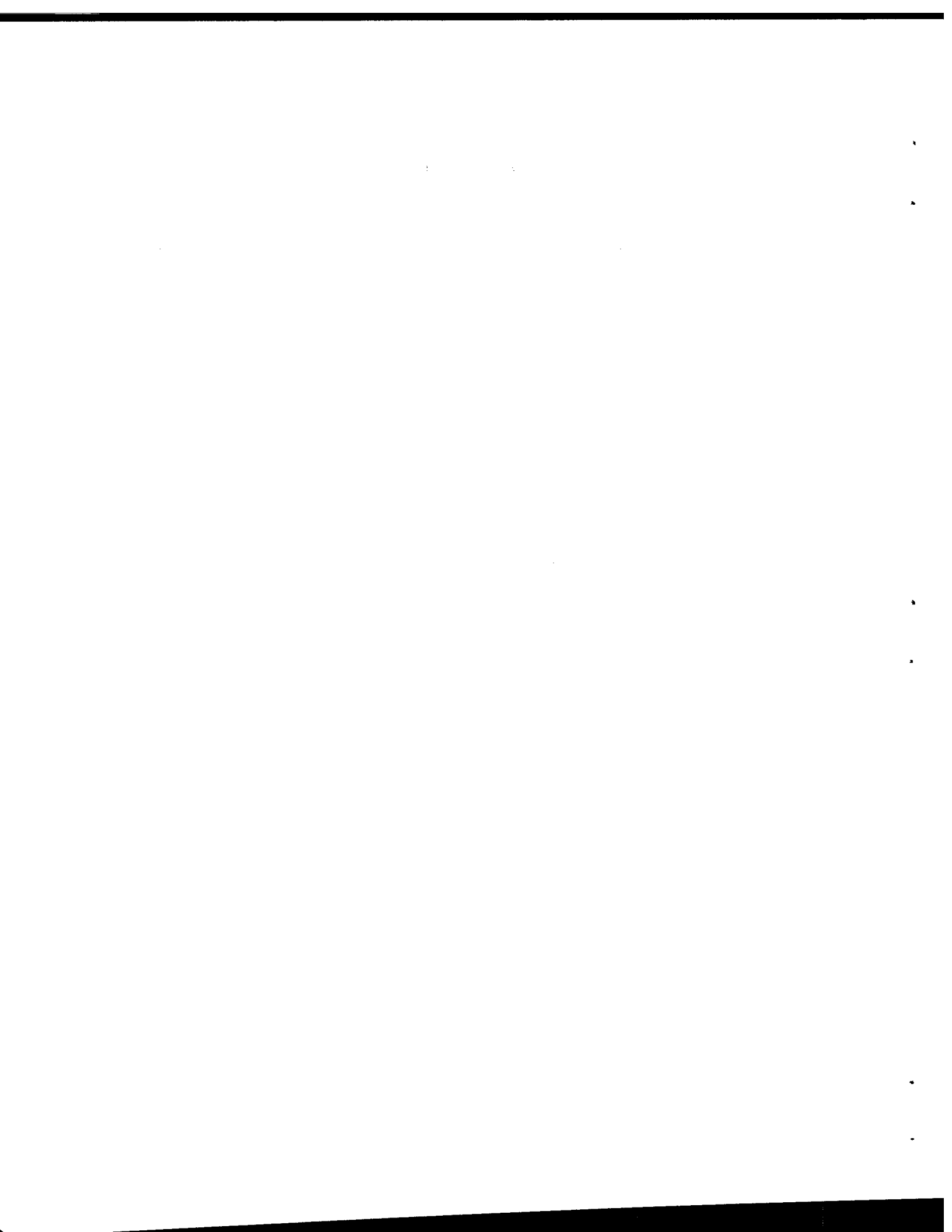


## TABLE OF CONTENTS

1.	Introduction .....	1
2.	Description of data and quality assessment .....	1
2.1	HFSWR data .....	1
2.2	Data quality .....	2
2.2.1	60 Hz harmonics interference and ADC bias.....	3
(a)	60 Hz harmonics .....	3
(b)	ADC bias .....	5
2.2.2	Loss of synchronization .....	6
2.2.3	Bad data points .....	6
2.3	NORDCO processing procedures .....	6
2.3.1	Band-pass filter .....	6
2.3.2	Mixing .....	8
2.3.3	Low-pass filter .....	11
2.3.4	Scaling .....	12
3.	In-house pre-processing software development. ....	12
3.1	Alternative pre-processing algorithm .....	14
3.1.1	Combining the band-pass and low-pass filters .....	14
3.2	Development of software for array processor .....	17
4.	Preliminary data analysis .....	17
4.1	Suppression of 60 Hz harmonic interference .....	18
4.2	Reconstruction of the 60 Hz Harmonics .....	21
4.3	Preliminary data analysis .....	24
4.3.1	Bragg lines of sea clutter .....	26
4.3.2	Observation of sky wave interference .....	26
4.3.3	Noise spectral density .....	28
4.4	Detection of ship and aircraft targets .....	32
4.4.1	Ship detection .....	32
4.4.2	Aircraft detection .....	34

Table of contents (Cont'd)

5.	Conclusion .....	36
5.1	Summary .....	36
5.2	Plans for analysis .....	36
	(a) Noise statistics .....	36
	(b) Sea-clutter statistics .....	37
	(c) Time-domain behaviour of sea clutter .....	37
	(d) Target detection .....	37
6.	References .....	38
7.	Acknowledgement .....	39
8.	Appendix A: FORTRAN programs for data pre-processing .....	40

## LIST OF FIGURES

Figure 1.	A typical returned waveform of an HFSWR pulse. ....	4
Figure 2.	Magnified version of the waveform of Figure 1. ....	4
Figure 3.	Typical spectrum of a HFSWR time series having 60 Hz power source harmonic modulation. ....	5
Figure 4.	Returned waveform of fifteen HFSWR pulses showing missing data. ....	7
Figure 5a.	Impulse response of the NORDCO digital band-pass FIR filter. ....	9
Figure 5b.	Frequency response of the NORDCO digital band-pass FIR filter. ....	9
Figure 6a.	Spectrum of a typical returned waveform of an HFSWR pulse. ....	10
Figure 6b.	Spectrum of the returned waveform of an HFSWR pulse after band-pass filtering. ....	10
Figure 7.	Spectrum of the returned waveform of a HFSWR pulse after mixing. ....	11
Figure 8a.	Impulse response of the NORDCO digital low-pass FIR filter. ....	13
Figure 8b.	Frequency response of the NORDCO digital low-pass FIR filter. ....	13
Figure 9.	Frequency response of a 320-stage FIR filter formed by cascading the NORDCO low-pass filter and the low-pass equivalent of the band-pass filter. ....	15
Figure 10.	Schematic diagram of the modified digital demodulation process for the HFSWR data. ....	15
Figure 11a	Average spectrum of a HFSWR time series produced using the NORDCO demodulation procedure. ....	16
Figure 11b	Average spectrum of a HFSWR time series produced using the modified demodulation procedure.....	16
Figure 12a	Waveform of a signal composed of 60 Hz harmonics. ....	22
Figure 12b	Construction of a full cycle of the harmonic waveform by combining segments sampled at regular intervals.....	22

LIST OF FIGURES (Cont'd)

Figure 13a	Reordering of HFSWR data segments to form a full cycle of the 60 Hz harmonic waveform. ....	23
Figure 13b	Determination of the instantaneous frequency of the power source harmonics. ....	23
Figure 14.	A typical HFSWR spectrum showing the Bragg lines and second order sea clutter components. ....	25
Figure 15.	Spectral power of the Bragg lines as a function of range index. ....	27
Figure 16.	Spectral power of the sea-clutter continuum as a function of range index. ....	28
Figure 17a.	I-channel waveform of a HFSWR time series during a period of moderate sky-wave interference. ....	29
Figure 17b.	I-channel waveform of a HFSWR time series during a period of severe sky-wave interference. ....	29
Figure 18a.	Spectrum of the HFSWR time series of Figure 17a. ....	30
Figure 18b.	Spectrum of the HFSWR time series of Figure 17b. ....	30
Figure 19.	Noise density of HFSWR signal as a function of range index. ....	31
Figure 20.	Data requirement for negligible transient effects from the 160-stage FIR filter. ....	33
Figure 21.	Spectrum of a HFSWR time series containing echoes from the CFAV Bluethroat. ....	34
Figure 22.	Spectrum of a HFSWR time series containing echoes from an Aurora aircraft. ....	36

## 1. Introduction

An experimental High Frequency Surface Wave Radar (HFSWR) project was carried out by NORDCO Limited of Newfoundland under contract to DND in 1989. The purpose of this project was to obtain some first hand experience in the data collection, processing and target detection using HF surface wave transmission. As a result, a substantial amount of HFSWR data were collected, but only a small portion of these data had been analyzed by the contractor. These data are brought back to the Radar Division of DREO. It is intended to analyze these data in-house so as to gain some insight into the characteristics of HF sea clutter, noise and various types of targets. Since these are raw data, they require some pre-processing before they can be analyzed. This report documents the development of in-house pre-processing software and the findings during preliminary examination of these data.

## 2. Description of data and quality assessment.

### 2.1 HFSWR data

The HFSWR data described herein were collected by NORDCO in 1989. The transmitter employed was the LORAN A located at Cape Bonavista, Newfoundland. This transmitter has a peak power of 1 MW, operating at a frequency of 1.95 MHz. The radar transmits a train of pulses (50  $\mu$ sec raised cosine waveform) at a PRF of 25 Hz. The receiving system comprised an 11-element array of doublet antennas, Steinbrecher 1630A receivers and associated signal processing and data acquisition systems. The element spacing is half wavelength (at 1.95 MHz), yielding a beamwidth of about 10°. Details of this facility may be found in [1].

Beam forming is performed at radio frequency (r.f) with signals from all antennas summed coherently. A beam pointing at a direction 110° clockwise from north results. The combined signal is first converted to an intermediate frequency (i.f.) of 25 kHz, band-pass filtered and sampled at a rate of 125 kHz. Sixteen bit analog-to-digital converters (ADC) are employed which provided a dynamic range of 96 dB.

In subsequent discussions, the term "range cell" is used to describe a distance in range determined by  $c\tau/2 = 7.5$  km where  $c$  is the speed of light and  $\tau$  is the radar pulse length. The numbers in the data records are called "range samples". A sampling rate of 125 kHz (or 8  $\mu$ sec per sample) corresponds to an inter-sample distance of 1.2 km. Hence the radar waveform is being over sampled because each range cell is covered by 6.25 range samples. This is done in order to provide a means to refine the range resolution of the radar through interpolation of range samples. Improved range resolution can be achieved if there is only one target per range cell at a given Doppler.

The data are stored in fixed length records on 8 mm EXABYTE cassettes. The data files on a cassette are read into the Radar Division's VAX-3800 computer for preliminary analysis. Each data record contains 512 two-byte integers. It is noted that the VAX computer stores the two bytes of a 16 bit word read from a tape in an order reversed from that of the computer which produced the tapes. The two bytes that make up a 16 bit word must be interchanged to obtain valid data in the VAX. This is easily done by executing an 8-bit circular shift of each integer read from the tape.

The first integer in each record is not used, while the second and third integers are used to indicate the pulse index and the number of range samples in the record, respectively. The remaining numbers in each record, beginning with the 4th value, are sampled returns of each transmitted pulse. The 4th value of each record corresponds approximately to the first range sample following the transmitted pulse (about 7.5 km). However, it was observed that the 4th and 5th values of some records may be invalid (e.g., 0 and 32767). These values indicate a condition of turn-on transient of the gating signal that enables the sampling. Consequently, the first valid sample of each record starts at the 6th value, representing a range of approximately 10 km. The last (512nd) value represents the radar return from a range of about 617 km.

## 2.2 Data quality

Most data files contain the returns of approximately 30,000 pulses (1200 seconds). With 512 range samples, such a file will occupy approximately 30 Mbytes of memory. Several deficiencies have been observed regarding the data.

### 2.2.1 60 Hz harmonics interference and ADC bias.

Figure 1 shows a typical returned waveform of an HFSWR pulse. At long ranges the return is composed mainly of noise (both atmospheric and receiver noises) which is a zero-mean process. One thus expects to observe small sample values fluctuating around zero at long ranges. Figure 2 is a magnified version of Figure 1. This sampled waveform clearly shows a positive bias with a segment of some time varying waveform superimposed. This waveform is identified as that of a 60 Hz power source harmonic interference.

#### (a) 60 Hz harmonics

There are two components of the power source harmonic interference. The first is multiplicative (modulation), and the second is additive. The time varying waveform observed in the data samples is the additive harmonic component. The multiplicative 60 Hz harmonic component is observed after the time series of the returns from individual ranges are formed. Figure 3 shows the spectrum of a typical time series. It can be seen that, besides the expected sea-clutter spectrum centered about zero-Doppler, there also exist similar spectral components at  $\pm 5$  Hz and  $\pm 10$  Hz. These spectral replica are the result of modulation of the radar signal by 60 Hz harmonics. Because of the low PRF (25 Hz) employed, the spectral replica that should have appeared at  $\pm 60$ ,  $\pm 120$ ,  $\pm 180$  Hz, etc. are aliased onto the  $\pm 5$  Hz and  $\pm 10$  Hz regions. These would be identical replica (except for a scaling factor) of the spectral component at zero-Doppler if the frequency of the power source is constant and the amplitudes and phases of its harmonics are also constant.

The additive component does not pose a serious problem since it will be removed by filters. The modulation component, however, will cause difficulties in detecting high speed targets. Consider a Mach 1 (330 m/sec) target. The Doppler shift of this target is 4.29 Hz. Since the PRF of the radar is 25 Hz, the 60 Hz harmonics are under-sampled, resulting in the signal spectrum being replicated at 5 Hz intervals. Thus a Mach 1 target will appear at a Doppler frequency that is occupied by the clutter (both sea and ground) modulated by the second harmonics (+ 5 Hz).

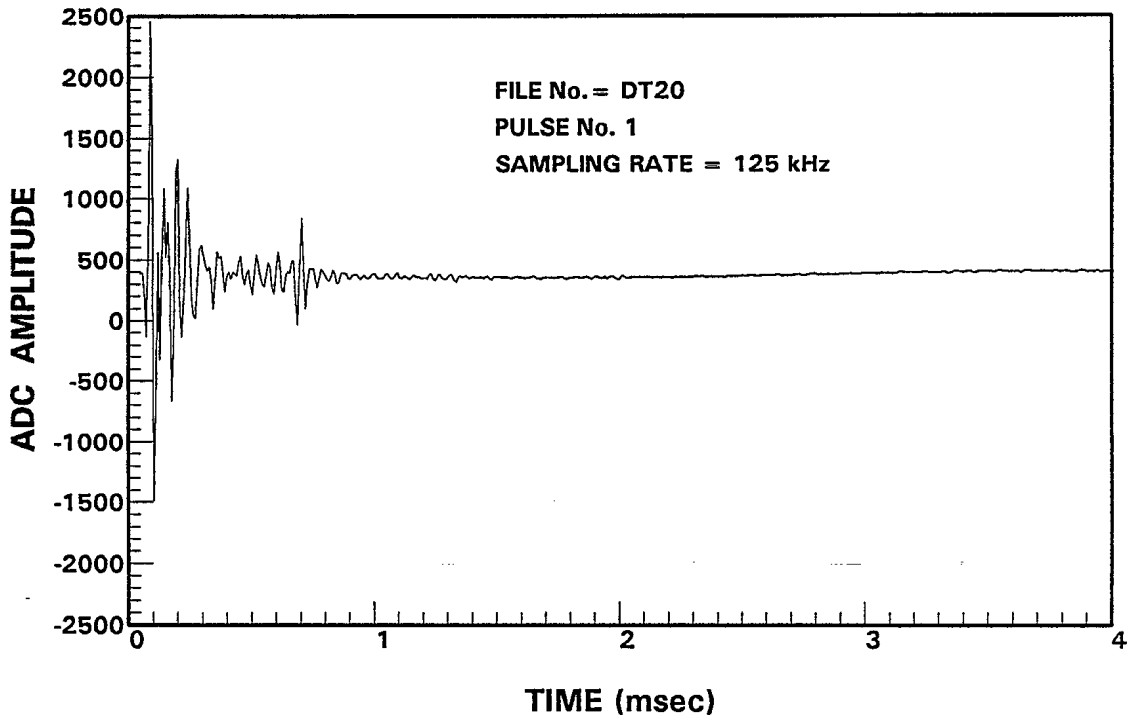


Figure 1. A typical returned waveform of an HFSWR pulse.

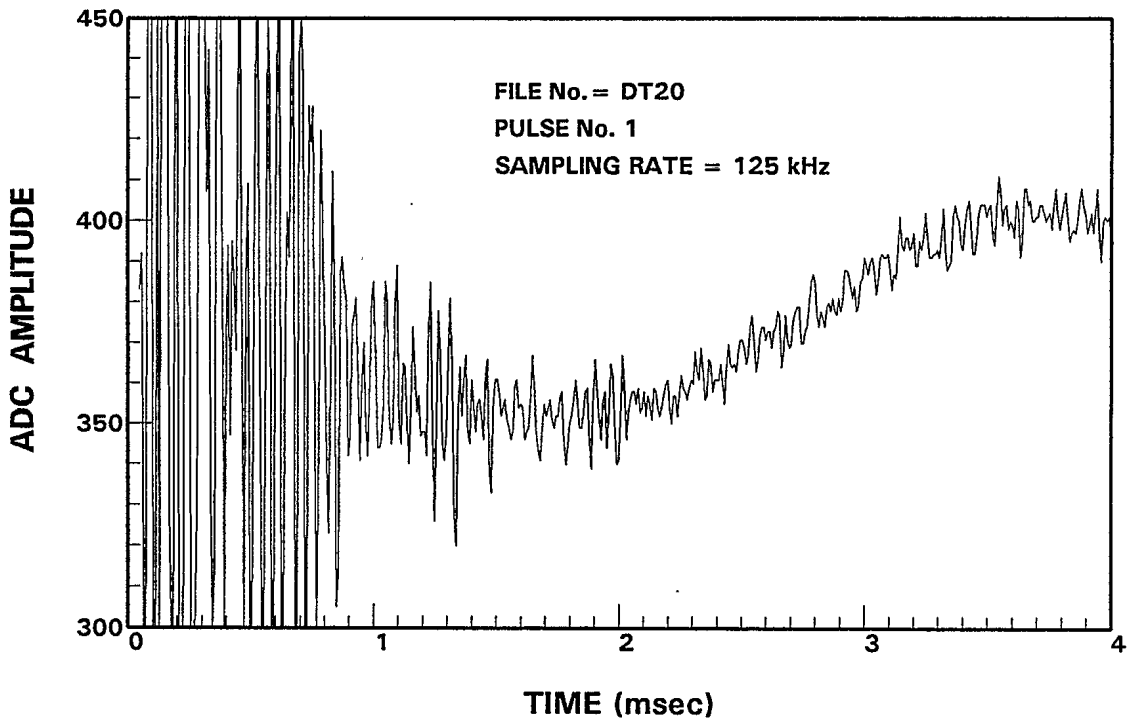


Figure 2. Magnified version of the waveform of Figure 1.

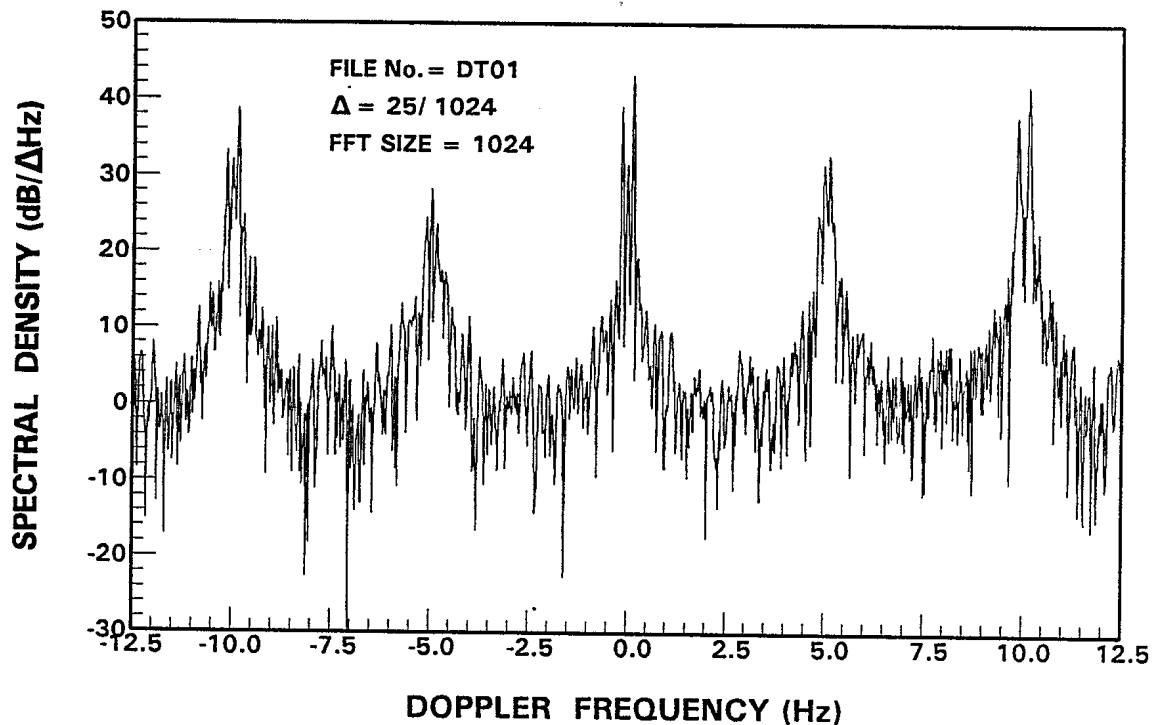


Figure 3. Typical spectrum of an HFSWR time series having 60 Hz power source harmonic modulation.

(b) ADC bias

The value of the DC bias in the ADC is approximately 360 and remains fairly constant from one data file to the next. The range of values for a 16-bit ADC is  $\pm 32767$ . Hence an offset of 360 in the ADC output represents 0.55 % of the full dynamic range. This bias will not normally present any problem because it can be removed by the band-pass filter. A band-pass and a low-pass, digital, finite impulse response (FIR) filter were employed by NORDCO in the demodulation of the HFSWR signal. Because the registers of the FIR filters are normally at zero state in the absence of any input, a dc component in the signal being filtered is equivalent to a large step function. Filtered outputs corresponding to the close-in range cells will be subjected to the filter's transient response to this step function. Since the DC offset is a constant, it can be subtracted from the data before any filtering is performed.

### 2.2.2 Loss of synchronization

Occasionally, a record may contain data that are out of sequence. This condition may be identified by observing the additive 60 Hz harmonic waveform in each record. Figure 4 shows the returns of 15 consecutive pulses. The scale of the plot is chosen so that the additive 60 Hz harmonic waveforms are clearly shown. As will be illustrated in Section 4.1, the 60 Hz harmonic waveform repeats itself cyclically every five pulses (see Figure 4). This cyclic pattern is sometimes interrupted by a data record that does not contain valid radar data. The waveform representing the return of the 352nd and 354th pulses are two such examples. It is observed that, in each data file, there exist up to several tens of segments in which this cyclical pattern is broken. This results in discontinuities in the time series. These discontinuities may be screened and replaced with sample values obtained by using interpolation. If there are too many discontinuities in a data segment, it could present problems in subsequent spectral analyses.

### 2.2.3 Bad data points

Occasionally, a data record contains sample values that are obviously incorrect. For examples, values of  $\pm 32767$  would indicate a saturated ADC condition. The origin of these bad data samples are not well understood. Inclusion of these bad data values would cause the noise floor to rise when spectral analysis is performed. The processing software flags such events so as to exclude these data samples from subsequent analysis. It is also possible to replace these samples with values interpolated from the valid samples that come before and after the bad data samples.

## 2.3 NORDCO processing procedures

The raw data must be processed to yield an equivalent complex baseband time series for subsequent spectral analysis. The processing procedure implemented by NORDCO consists of (i) band-pass filtering, (ii) mixing and (iii) low-pass filtering.

### 2.3.1 Band-pass filter

The purpose of the band-pass filter is to suppress the noise in the frequency region outside the signal bandwidth. To a certain extent, this had already been done by the

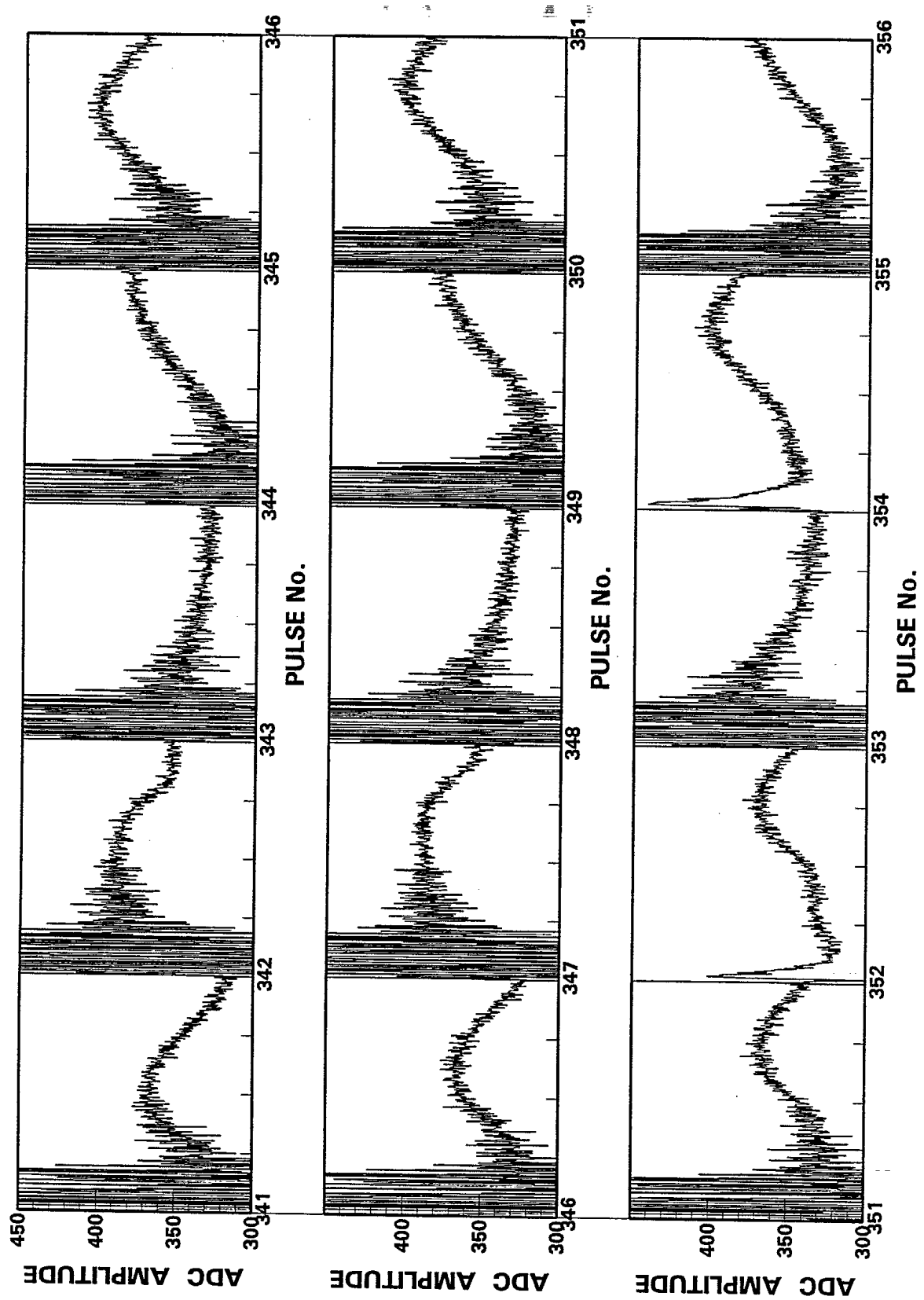


Figure 4. Return waveform of 15 consecutive HFSWR pulses showing missing data.

analog low-pass filter (called anti-aliasing filter) at the 25 kHz i.f. The digital band-pass filter used by NORDCO was a 160-stage finite impulse response (FIR) filter with a mid band frequency of 25 kHz and cutoff frequencies of 15 kHz on either side of mid band. The filter coefficients are reproduced in this report using the FORTRAN program described in [2] with the following set of input parameters:

	Band 1	Band2	band 3
frequency at lower band edge	0.0	0.08	0.35
frequency at upper band edge	0.05	0.32	0.5
desired value	0.0	1.00	0.0
weighting	100.	1.00	100.

The cutoff frequencies are normalized with respect to the sampling rate. For example, a normalized frequency of 0.5 represents 62.5 kHz.

The impulse response and the corresponding frequency response of this band-pass filter are shown in Figure 5a and 5b, respectively. The spectrum of a typical returned waveform of a transmitted pulse is shown in Figure 6a. This spectrum is computed by performing a 1024 point FFT on the samples in a data record (507 samples padded with trailing zeros to make a 1024 point array). After band-pass filtering, the signal spectrum is as that shown in Figure 6b. It can be seen that there is still a significant residue at zero frequency which is the consequence of the ADC offset.

### 2.3.2 Mixing

The purpose of mixing is to shift the signal spectrum down to complex baseband so as to extract the phase information of the returns with respect to the transmitted pulse. Since the recorded data were sampled at 125 kHz, which is an integer multiple of the carrier frequency of 25 kHz, the 25 kHz local oscillator and the clock that triggered the sampling were synchronized to the same stable source. At this sampling rate (1 sample per 8  $\mu$ sec) each cycle of the 25 kHz carrier consists of 5 values:

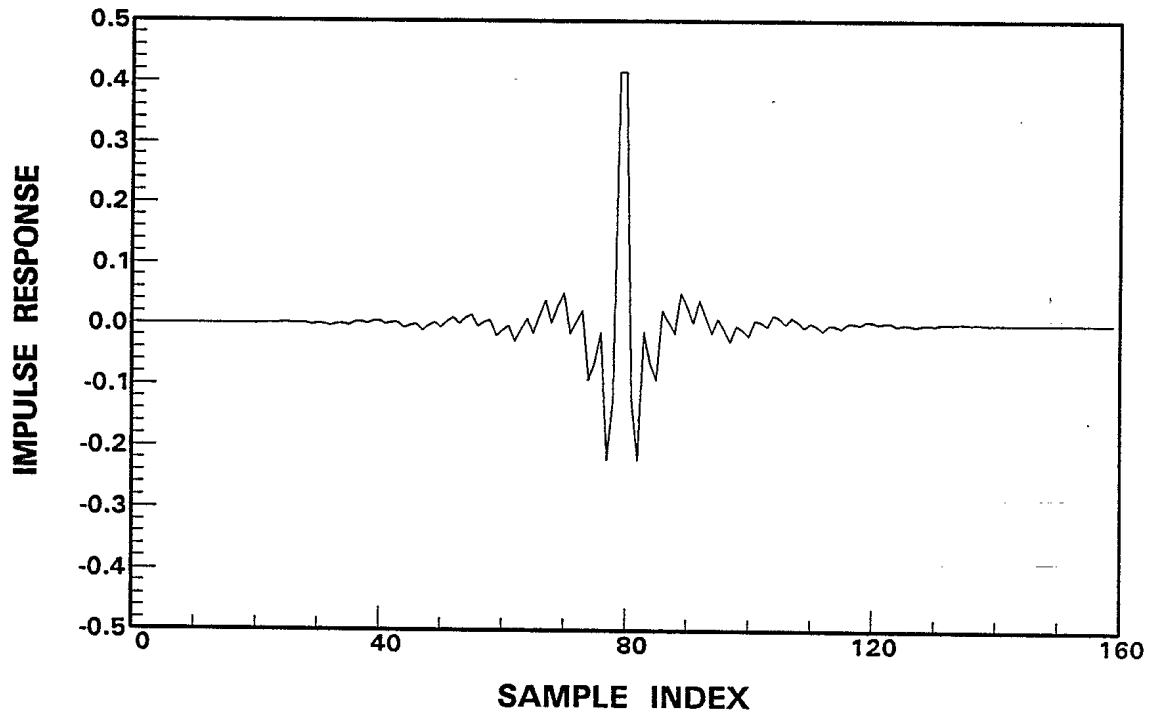


Figure 5a. Impulse response of NORDCO FIR band-pass filter.

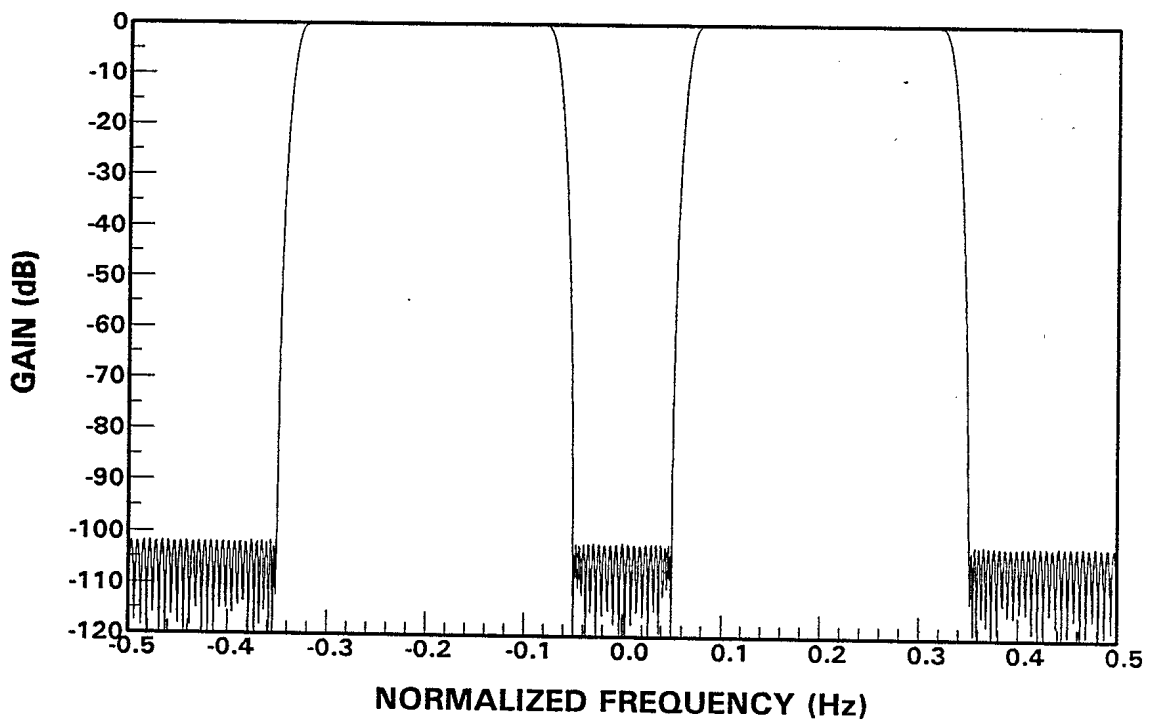


Figure 5b. Frequency response of NORDCO FIR band-pass filter.

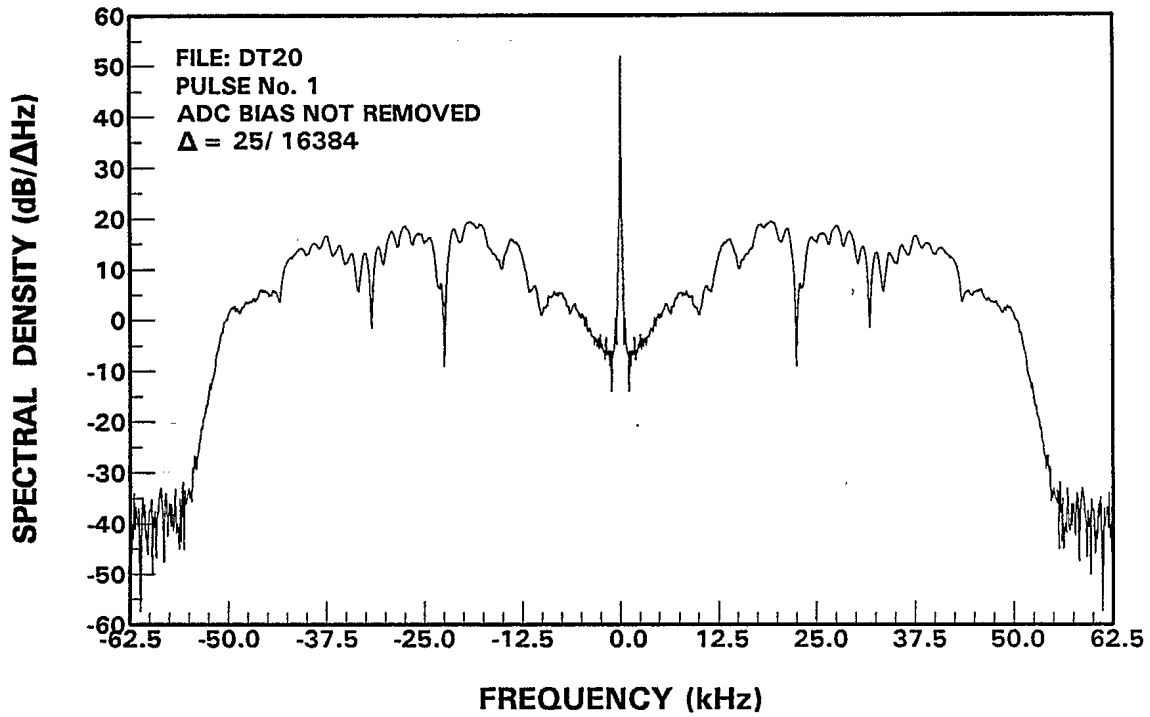


Figure 6a. Spectrum of a typical returned waveform of an HFSWR pulse.

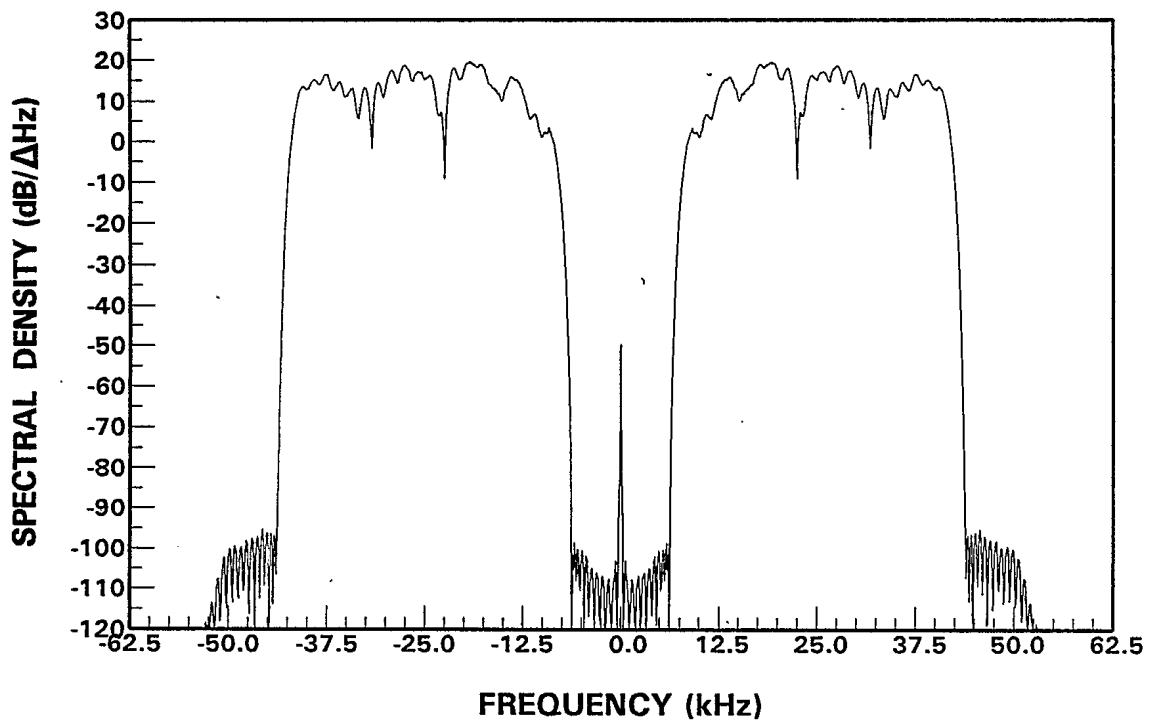


Figure 6b. Spectrum of the returned waveform of an HFSWR pulse after band-pass filtering.

In-phase:  $\cos(0), \cos(2\pi/5), \cos(4\pi/5), \cos(6\pi/5)$  and  $\cos(8\pi/5)$   
Quadrature:  $\sin(0), \sin(2\pi/5), \sin(4\pi/5), \sin(6\pi/5)$  and  $\sin(8\pi/5)$ .

The mixing process is accomplished by multiplying contiguous sets of 5 data samples by the above sets of values. After mixing, the spectrum of the waveform is that shown in Figure 7.

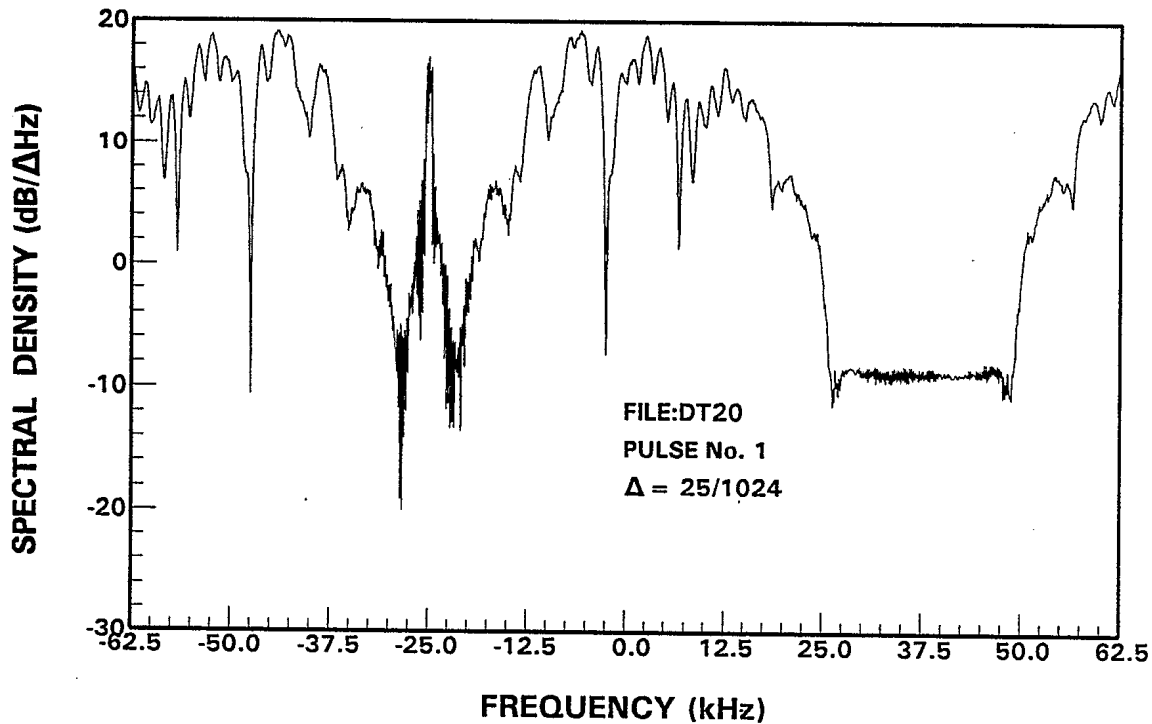


Figure 7. Spectrum of the returned waveform of an HFSWR pulse after mixing.

### 2.3.3 Low-pass filter

Low-pass filtering is used to eliminate the spectral replica of the signal centered about a frequency that equals twice the i.f. frequency (in this case, 50 kHz). This component results from a product of two sinusoidal functions (see Figure 7). In addition, after demodulation, a matched filter is usually required to maximize the signal-to-noise ratio for the particular transmitted waveform. NORDCO used a low-pass filter that has

the same bandwidth as the transmitted waveform to fulfill both purposes since the precise shape of the received waveform is not very well defined. This filter is also a 160-stage FIR filter with a cutoff frequency at 10 kHz. The coefficients of this filter are obtained by running the FIR design program as in the band pass filter case, except the input parameters are:

	band 1	band 2
frequency at lower band edge	0.0	0.11
frequency at upper band edge	0.08	0.5
desired value	1.00	0.0
weighting	1.00	100.

The impulse response and the frequency response of the low-pass FIR filter are shown in Figures 8a and 8b, respectively. Two identical low-pass filters are required, one for the I-channel and one for the Q-channel.

### 2.3.4 Scaling

The digital filters should have a unity gain within the passband. Filters designed using the FORTRAN program described in [2] are not normalized to provide a unity gain at mid-band. Consequently, a scaling factor may be required to provide numerically correct results in computing parameters such as sea-clutter spectral power and noise power, etc.

### 3. In-house pre-processing software development.

A software based on the project report [1] produced by NORDCO was first implemented in the RADAR Division's Vax 3800 computer. It becomes evident that the required processing to convert the raw data into complex baseband time series is rather time-consuming. Some effort has been devoted to devising means to reduce the required processing time. Two approaches are taken: (a) improving existing algorithm and (b) utilizing the in-house array processor hardware.

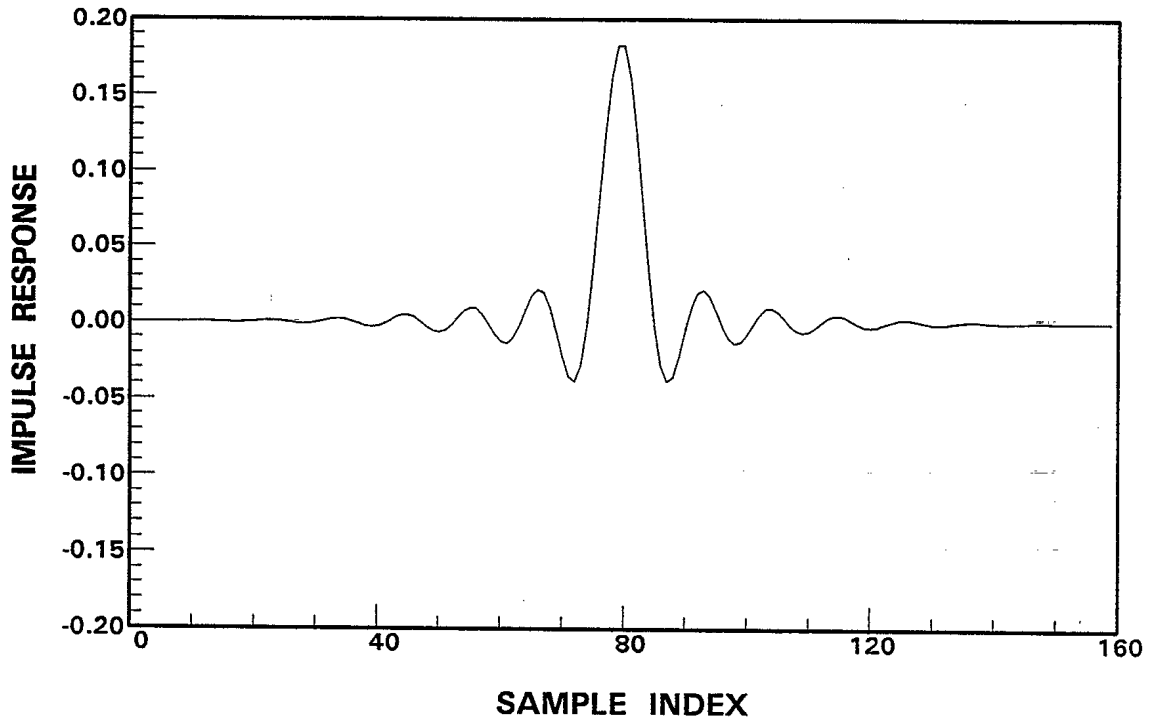


Figure 8a. Impulse response of NORDCO FIR low-pass filter.

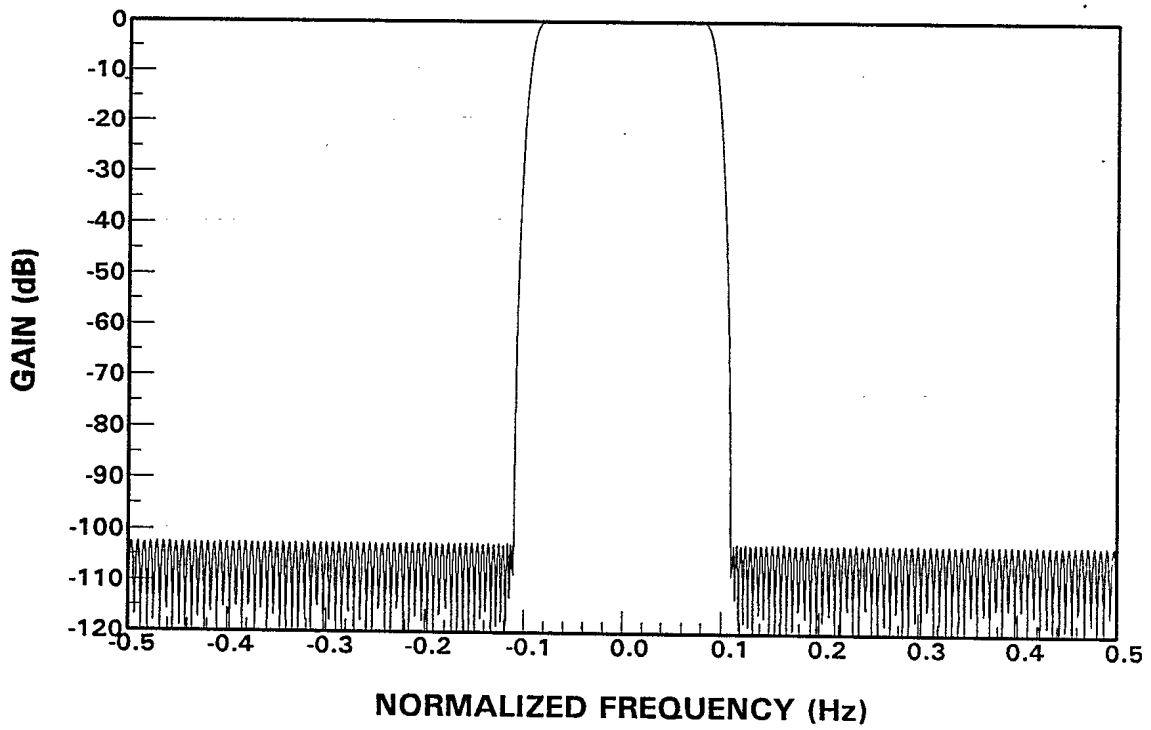


Figure 8b. Frequency response of NORDCO FIR LOW-pass filter.

### 3.1 Alternative pre-processing algorithm.

The processing procedure employed by NORDCO was presented in Section 2.3. In this section we shall examine various ways to improve the pre-processing algorithm.

#### 3.1.1 Combining the band-pass and low-pass filters.

Since the data will eventually be converted to the equivalent complex baseband, the band-pass filtering operation can also be performed at complex baseband. At first glance, it would appear some saving may be realized if both the band-pass and low-pass filters were combined into a single filter with a transfer function that is equal to the product of those of the low-pass filter and the low-pass equivalent of the band-pass filter. However, this requires an FIR filter that is twice as long (i.e. 320 stages) as the original filters. Since in complex baseband, the I- and Q-channel data are filtered separately as opposed to a single channel at i.f., combining the two filters actually requires more processing.

The frequency response of a filter formed by cascading the low-pass filter (Section 2.2.3) and the low-pass equivalent of the band-pass filter (Section 2.2.1) is shown in Figure 9. Theoretically, it provides more than 200 dB of attenuation outside the pass-band. However, since the dynamic range of the data is only 96 dB (16-bits), it is questionable that such a large attenuation would make any significant difference in the results compared with those obtained with a filter that has a moderate attenuation.

It is decided to eliminate the band-pass filter altogether and use the low-pass filter only. The simplified digital demodulation process of the NORDCO data is shown in Figure 10. The ADC bias is first subtracted from the data. The results are multiplied with the I- and Q- channel mixer samples to form the I- and Q- channel samples. The I- and Q- sequences are then low-pass filtered separately to yield the required complex time series.

The subtraction of the ADC offset and the elimination of the band-pass filter provide the benefits of requiring fewer operations and reducing the effect of the transient response due to the step function. Figures 11a and 11b show the averaged spectra of the time series of a close-in range cell (the 10th cell from start), obtained by using the

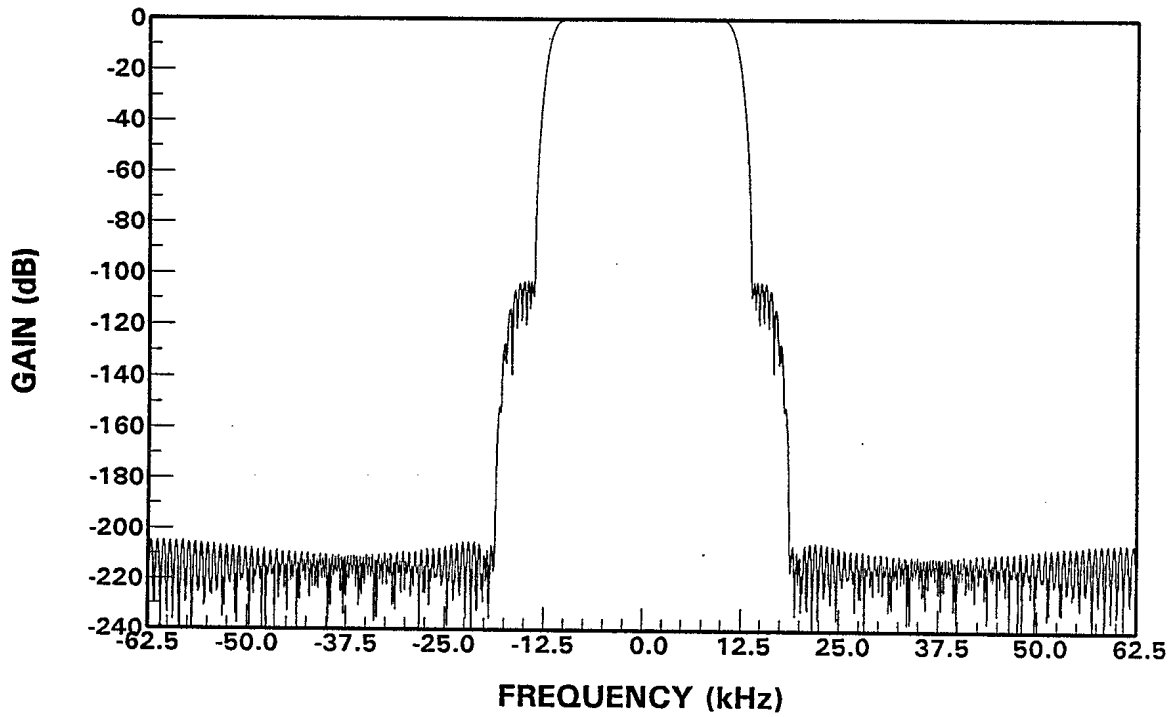


Figure 9. Frequency response of a 320-stage FIR filter formed by cascading the NORDCO low-pass filter and the low-pass equivalent of the band-pass filter.

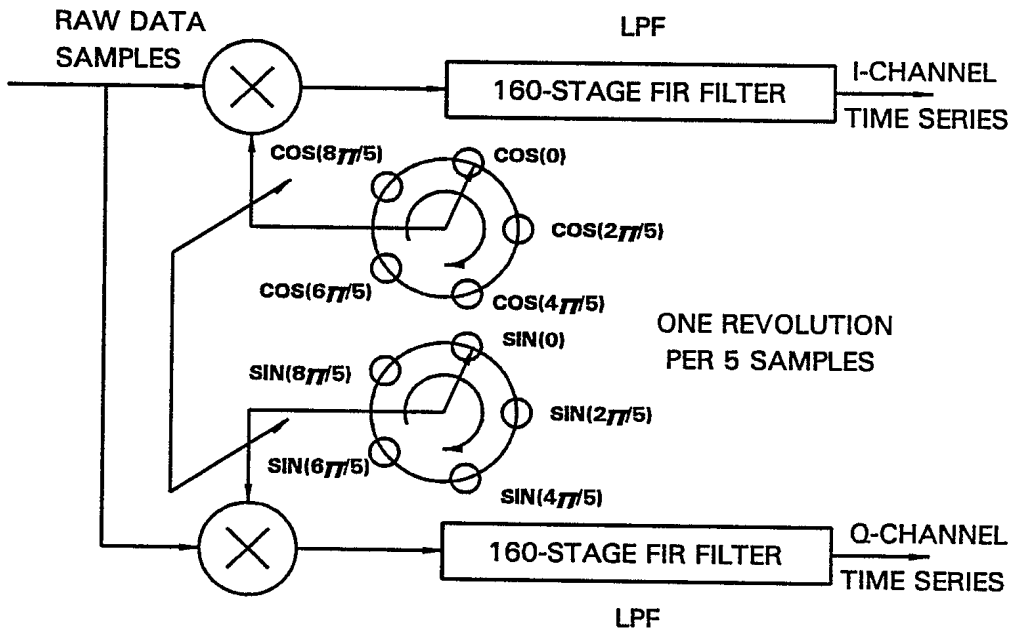


Figure 10. Schematic diagram of the modified digital demodulation for the HFSWR data.

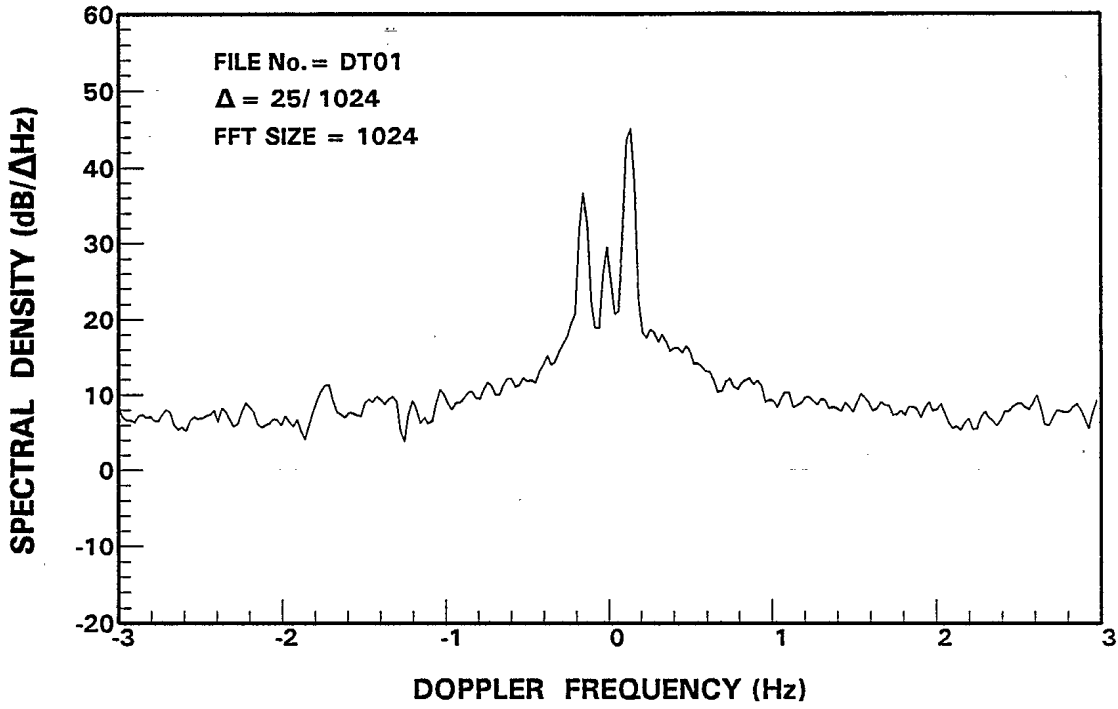


Figure 11a. Spectrum of time series obtained using the NORDCO demodulation procedure.

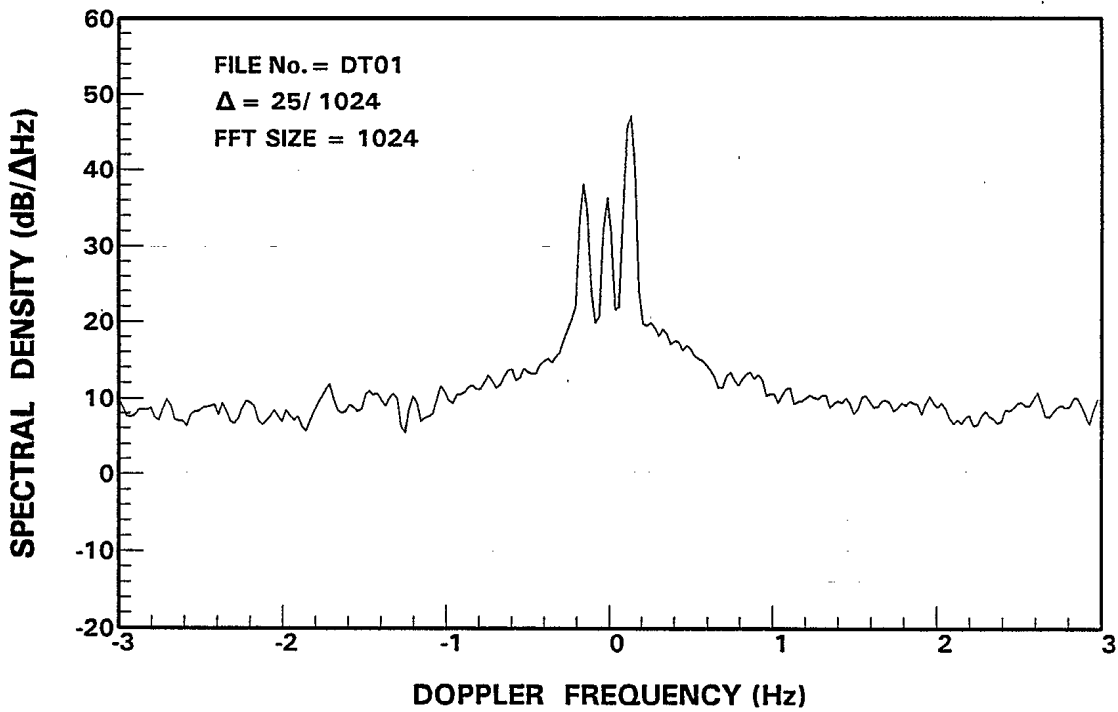


Figure 11b. Spectrum of time series obtained using the modified procedure.

NORDCO procedure and the procedure described in this Section, respectively. It can be seen that, while the two spectra are similar, there is a significant difference in the zero-Doppler component. This discrepancy is not observed in spectra for range cells at longer ranges which led us to believe that it was the result of transient effect of the ADC offset.

### 3.2 Development of software for array processor.

Significant saving in processing time can be achieved if the data pre-processing is performed using the Floating Point Array Processor [3]. The Array Processor (AP) reduces data processing time by performing mathematical operations in a pipeline fashion. This means the overhead inherent in sequential computing machines is eliminated to a large extent. The software developed on the VAX 3800 has been translated into AP FORTRAN and Vector Function Chainer software [4].

It requires more than 8 hours of CPU time and more than 17 hours of elapsed time for the VAX computer to generate 500 time series (with 30,000 complex samples each). The CPU time required for the VAX is reduced to a negligible level; however, the elapsed time required is still substantial, about four hours. It appears that the processing time is I/O (reading and writing to disks) limited. The source codes of the calling program and subroutines are shown in Appendix A.

### 4. Preliminary data analysis

As discussed in Section 1, the objective of analyzing these data in-house is to gain some insight in HFSWR sea clutter, noise and target detection characteristics. One important piece of information that we hope to get from these data is the probability density function of the noise and sea clutter after various signal processing (e.g. after the FFT). The knowledge of the residual clutter and noise characteristics is important in determining the appropriate detection threshold with an acceptable probability of false alarm.

Normally, it is a straightforward process to acquire this knowledge from the data. One can form histograms of the noise (or clutter) samples using the ensemble of the FFT output that corresponds to the various spectral regions of interest and determine the relative goodness of fit of the histograms to some known statistical models (e.g. Rayleigh, Weibull, Chi , etc). However the presence of the 60 Hz harmonics complicated matters. The noise and clutter statistics may be observed more easily if the effects of the 60 Hz harmonics can be suppressed. One possible way to accomplish this is outlined in section 4.1.

#### 4.1 Suppression of 60 Hz harmonic interference.

Any waveform that results from the summation of one or more harmonically related sinusoidal functions has a period less than or equal to that of the fundamental sinusoid. For example, if a waveform is formed from summing a 60 Hz sinusoid with an 180 Hz sinusoid, then the resulting waveform will repeat itself every  $1/60=16.6667$  msec.

We can represent the signal appearing at the ADC as follows:

$$r(t) = x(t) \left\{ 1 + \sum_{i=1}^M A_i(t) \cos(2\pi i f t + \phi_i(t)) \right\} + b(t) + d \quad (1)$$

where  $f$  is the fundamental frequency of the interfering harmonics;  $A_i$  and  $\phi_i$  are their amplitudes and phases.

Component  $b(t)$  is also composed of harmonics of the 60 Hz interference signal; however, this component is different from those of  $A_i$ 's in that it is added to the signal at the input of the ADC. Parameter  $d$  is the ADC bias.

Theoretically, one should be able to remove the interference components by obtaining estimates of parameters  $f$ ,  $A_i$ ,  $\phi_i$ ,  $b$ , and  $d$ . The ADC bias is easily estimated because it is a constant. The other parameters, however, are functions of time and therefore much more difficult to estimate.

The period of 60 Hz harmonics is 16.667 msec, and the radar's pulse repetition interval (PRI) is 40 msec. The smallest common denominator between these two numbers is 200 msec which represents the time required to transmit 5 pulses. This means that, if a sample of the interfering harmonics is taken at the time instant of the  $n$ th pulse transmission, the same value should occur at the time of pulse no.  $n+5$ . This assumes, of course, that the parameters of the harmonics are all constants. Unfortunately, as we shall see, the parameters of the harmonics do change over a finite interval of time.

The modulation of the received radar signal by the 60 Hz harmonics can occur almost anywhere along the receiver chain. For example, it could be present in the dc power supply, or it could be in the form of modulation in the local oscillator. Consequently, there is no assurance that the modulating 60 Hz harmonic waveform is identical to that of the additive component.

The relative amplitudes and phases of the additive 60 Hz harmonics do not seem to change at a fast rate as evidenced by the similarity of the waveforms at different times. The fundamental frequency of the interference sinusoids does fluctuate about 60 Hz randomly; however, this frequency fluctuation should be identical for the two sets of harmonics (additive and multiplicative). Consequently, it is possible to utilize the information provided by the additive 60 Hz harmonic components to estimate the parameters of the multiplicative 60 Hz harmonic components.

After mixing and low-pass filtering, the complex baseband signal may be represented as follows:

$$r_n = r(n\Delta t) = x(n\Delta t) \left\{ \sum_{i=-M}^M A_i \exp[j(2\pi ifn\Delta t + \phi_i(n\Delta t))] \right\} \quad (2)$$

where  $f = 60$  Hz, and any deviation of the frequency from 60 Hz is modeled as a time variation of the phase  $\phi_i$ ;  $A_0 = 1$  and  $\phi_0 = 0$ . We shall consider harmonics of order higher than  $M$  to be negligible.

Thus the samples without 60 Hz harmonic modulation are:

$$x_n = x(n\Delta t) = \frac{r_n}{\sum_{i=-M}^M A_i \exp[j(2\pi r_i n\Delta t + \phi_i(n\Delta t))]} \quad (3)$$

The discrete Fourier transform (DFT) of the time series  $x_n$  is:

$$F_k = \frac{1}{N} \sum_{n=0}^{N-1} x_n \exp(-j2\pi nk/N) \quad (4)$$

Since the effect of the 60 Hz harmonic modulation is to replicate the signal spectrum at  $\pm 5$  Hz and  $\pm 10$  Hz, the DFT of a time series that does not have any harmonic modulation will have only noise component in the spectral region around  $\pm 5$  Hz and  $\pm 10$  Hz. This provides a means to estimate the parameters  $A_i$  and  $\phi_i$  by using a constrained optimization technique [5]. Define an objective function  $P$  as:

$$P_{K_1, K_2} = \sum_{k=K_1}^{K_2} F_k^* F_k \quad (5)$$

where  $K_1$  and  $K_2$  are frequency indices that define a spectral region around  $\pm 5$  Hz and  $\pm 10$  Hz. Indices  $K_1$  and  $K_2$  are chosen such that the power of the main signal spectrum will be negligible in the spectral region defined by  $K_1$  and  $K_2$ . Over a finite time interval the relative amplitudes and phases of the harmonics may be considered constant. This time interval should be long enough to provide enough samples to perform a DFT. The appropriate values of  $A_i$  and  $\phi_i$  can be found by minimizing  $P$ , provided that the fundamental frequency of the interfering harmonics is known and is a constant.

As discussed earlier in this section, the frequency of most AC power sources does fluctuate about 60 Hz over short time intervals, depending on the loading condition and other factors. Consequently, the relative phase of the various harmonic components have become functions of time. This greatly complicates matters because the phases must now be represented by higher order polynomials.

#### 4.2 Reconstruction of the 60 Hz Harmonics.

In each data record, there are 512 samples. Since the sampling interval is 8  $\mu$ sec, each data record represents an observation interval of about 4 msec. The period of a 60 Hz harmonic waveform is nominally 16.667 msec. One can obtain a fairly good estimate of the additive harmonic waveform from 5 consecutive data records. Referring to Figure 12a, the waveform represents a function that is composed of harmonics of a 60 Hz sinusoidal function. Pulses 1, 2, 3, 4 and 5 are transmitted at 0, 40, 80, 120, 160 msec, respectively. Segments A, B, C, D and E represent the time intervals in which the return waveforms from pulses 1, 2, 3, 4 and 5, respectively, are sampled.

If the fundamental frequency does not deviate from 60 Hz significantly, the starting time instants for the returns of pulses 2, 3, 4 and 5 with respect to one cycle of the harmonic waveform that begins at time 0 are:  $\text{mod}(40,16.667) = 6.667$ ,  $\text{mod}(80,16.667) = 13.333$ ,  $\text{mod}(120,16.667) = 3.333$  and  $\text{mod}(160,16.667) = 10$  msec, respectively.

It is possible, by arranging the data segments in the following order: A, D, B, E and C, to construct a complete cycle of the interfering harmonics. Of course, the presence of the radar return poses a problem since the magnitudes of the radar returns from close-in range cells could be very large (due to Bragg resonance from sea clutter). Fortunately, there is a small overlap between successively data segments. For example, the tail portion of segment A overlaps the beginning portion of segment D (see Figure 12b). This permits the use of data segment that are free of sea clutter components in place of those with strong sea clutter components.

The reordered samples of five consecutive data records taken from file DT20 are shown in Figure 13a. A 32-point block averaging is performed on the data to eliminate the noise fluctuation. Further smoothing is obtained using a 3-point moving average.

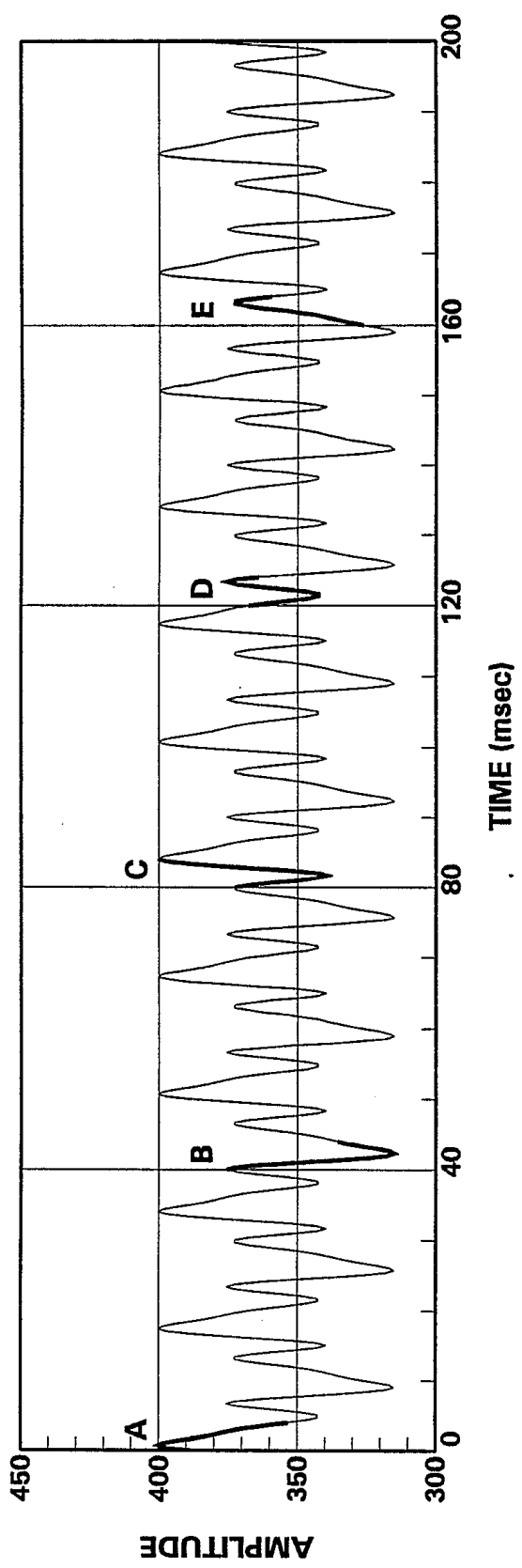


Figure 12a. Waveform of a signal composed of 60 Hz harmonics.

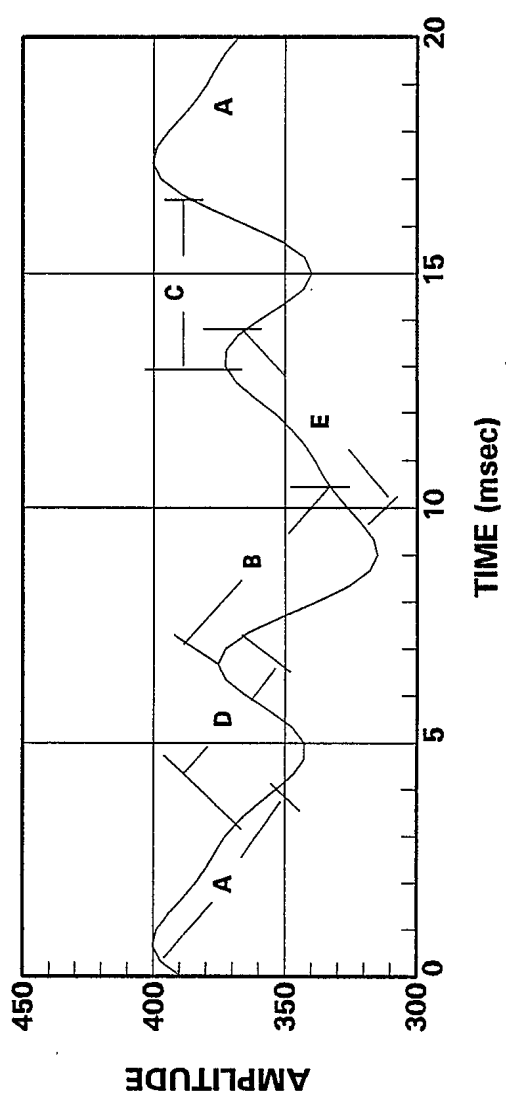


Figure 12b. Construction of a full cycle of harmonic waveforms by combining segments sampled at regular time intervals.

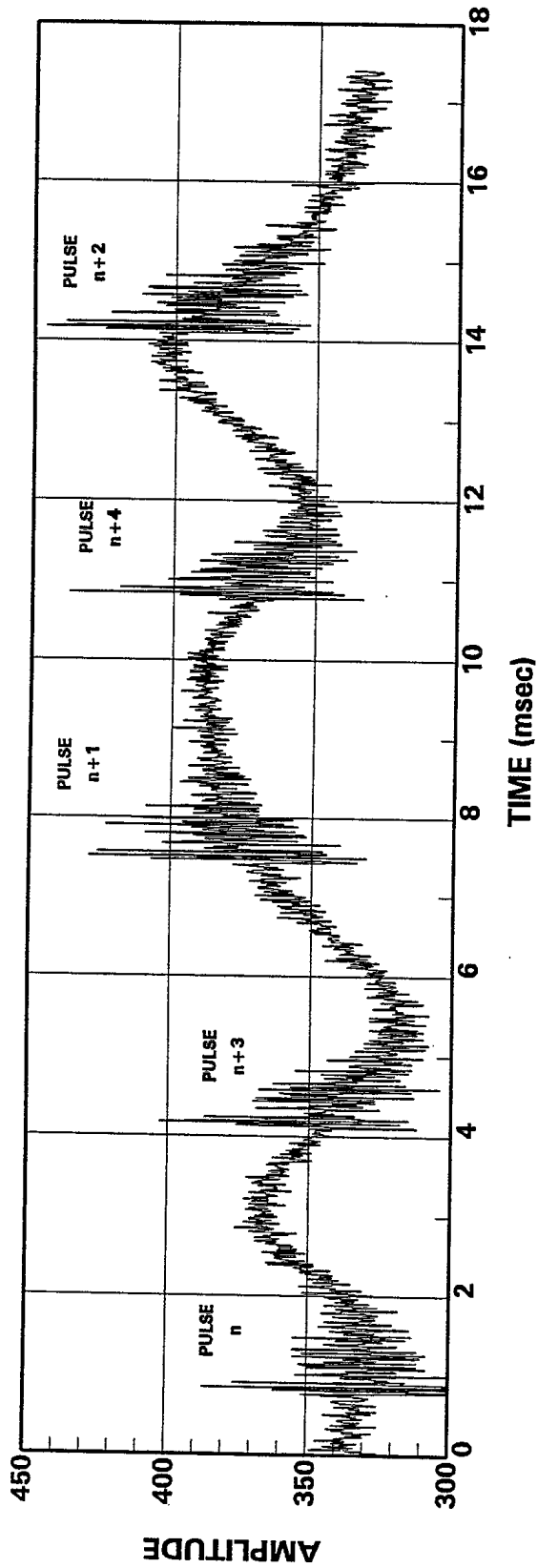


Figure 13a. Reordering of HF-SWR data segments to form a full cycles of 60 Hz harmonics.

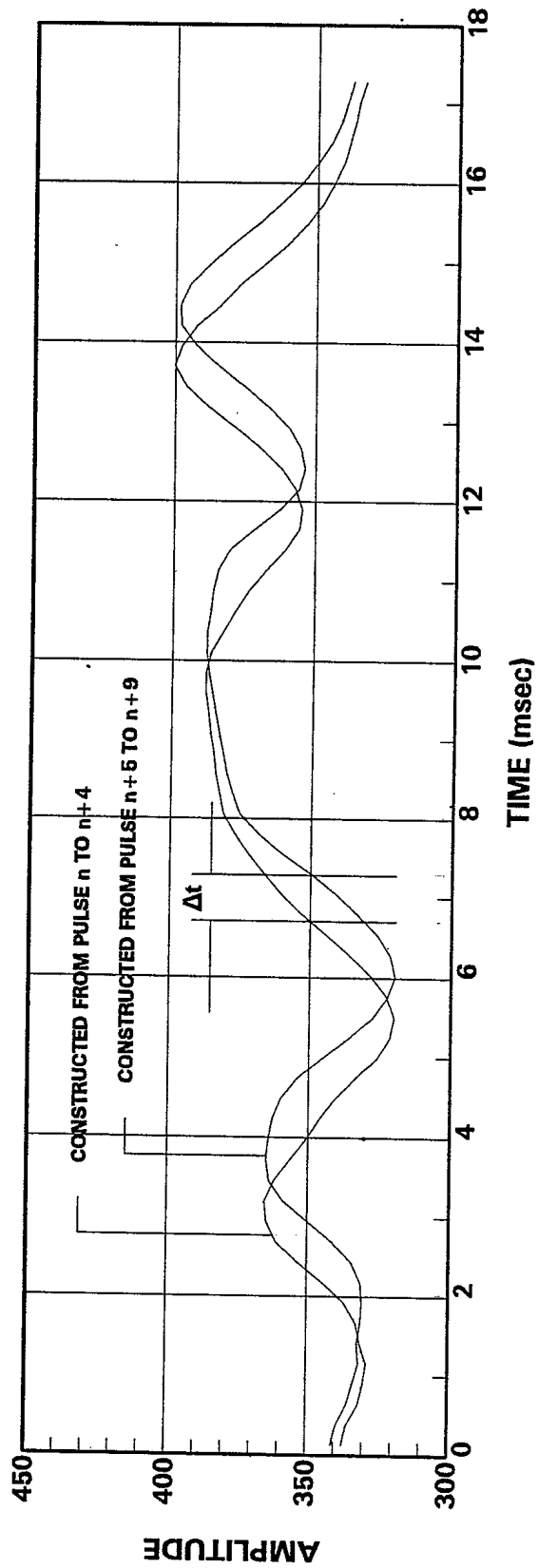


Figure 13b. Determination of the instantaneous frequency of the power source harmonics.

To obtain an estimate of the fundamental frequency of the interfering harmonics, one needs to compare the reconstructed waveforms from two successive sets of 5 pulses. If the fundamental frequency is exactly 60 Hz, the pattern of the interference should repeat every 5 pulses (200 msec). If, on the other hand, the fundamental frequency is slightly lower than 60 Hz, say 59.5 Hz, the waveform constructed from the next set of 5 pulses would be shifted to the right because it takes longer to complete a cycle.

Figure 13b shows two consecutive cycles of the reconstructed 60 Hz harmonics. Here  $\Delta t$  is the shift in time between two consecutive cycles of the 60 Hz harmonic waveform. Since it takes 200 msec to produce a shift of  $\Delta t$ , the shift in 16.667 msec (a period of 60 Hz) is  $16.667 \Delta t / 200$ . The instantaneous frequency estimate of the harmonic waveform is:

$$f = \frac{1}{16.6667 \times 10^{-3} \left( 1 \pm \frac{\Delta t}{200 \times 10^{-3}} \right)} = \frac{60}{1 \pm 5 \Delta t} \quad (6)$$

where the sign in the denominator of Eq (6) is determined from the sign of the time shift (+ for right shift and - for left shift) and  $\Delta t$  is in seconds.

We now have a time history of the instantaneous frequency of the fundamental sinusoid estimated every 200 msec. Within this time interval, we may consider the frequency to be constant. The interfering harmonics can be estimated using the procedure outlined in Section 4.1.

### 4.3 Preliminary data analysis.

Preliminary analysis has been carried out on several data files. Each data file was processed using the software described in Section 3.1 to yield a set of 507 (i.e.,  $512 - 5$ ) time series. A 16384-point FFT was performed on the time series using the first 16384 samples and a Blackman window [6]. A typical result is shown in Figure 14 for the time series of the 10th range sample of file DT24.

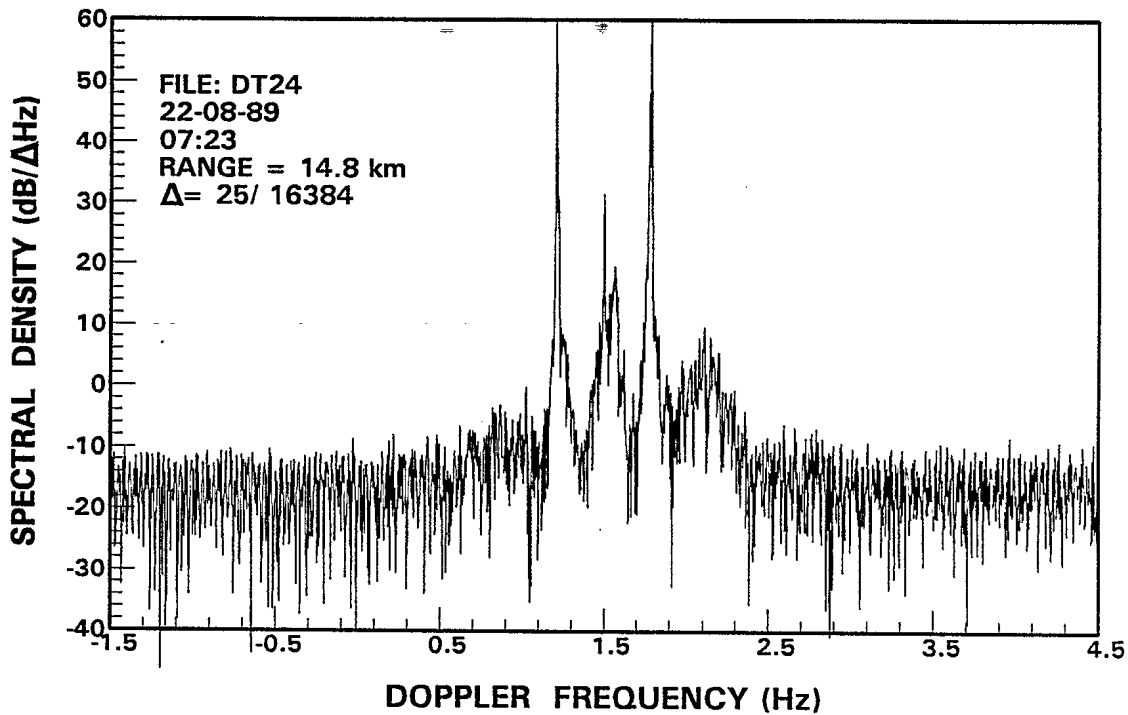


Figure 14. A typical HFSWR spectrum showing the Bragg lines and second order sea clutter.

The advancing and receding Bragg lines of the sea clutter are very prominent. The Doppler frequency of the advancing and receding Bragg lines are estimated to be 0.14 and 0.1388 Hz, respectively. The following four quantities are of interest: the power in the advancing and receding Bragg lines, the power in the sea clutter continuum and the noise spectral density.

It should be emphasized that, at the present time, we are only interested in the relative magnitudes of these quantities. Hence no attempt has been made to calibrate the data in terms of equivalent radar cross section (RCS). The calibration process involves the determination of a constant  $k_c$  such that the equivalent RCS of the echo from a given range cell is determined by:

$$\sigma_i = k_c(I_i^2 + Q_i^2) \quad (7)$$

where  $I_i$  and  $Q_i$  are the numerical I- and Q- values, respectively, of the the echo from that range cell for the  $i$ th pulse.

The calibration constant  $k_c$  is determined from the two way HFSWR radar equation [1] which takes account of parameters such as transmit power, antenna gains, propagation losses, filter gains, etc. The unit for RCS values is  $m^2$ . In subsequent discussions all spectral powers will be referenced to a numerical value of unity (or 0 dB). These quantities can be easily converted to the equivalent RCS values once the calibration constant is known.

#### 4.3.1 . Bragg lines of sea clutter.

The power spectral density of a signal is calculated from its periodogram [8] which is the squared magnitude of the FFT. The spectral power of the Bragg lines is estimated by summing the 16384 point periodogram over 11 Doppler samples surrounding the one that contains the Bragg peaks. Since the spectral resolution is  $25/16384 = 0.001526$  Hz, this represents the power in a spectral region of about 0.01526 Hz.

The power in the Bragg lines as a function of range for data file DT24 is shown in Figure 15. For this data file, the power in the receding Bragg lines is, on the average, a few dB lower than the power in the advancing Bragg line. They appear to decrease linearly (in dB scale) as a function of range. This apparent linearity in the decreasing power of the Bragg lines with respect to range is probably the result of the combined effects of the HFSW propagation loss and the increase of Bragg power with range due to increasing range cell size.

#### 4.3.2 Observation of sky wave interference

Besides the Bragg lines, HF sea clutter also comprises other spectral components, namely, those from second order scattering [8]. We shall call the spectral component of the sea clutter excluding those of the two Bragg lines the sea-clutter continuum. It was observed that at 1.95 MHz, the spectral extent of the sea clutter continuum is generally confined to  $\pm 0.5$  Hz.

The power of the sea clutter continuum is obtained by first integrating the periodogram over the spectral region between  $\pm 1$  Hz and subtracting the power of the Bragg lines. The  $\pm 1$  Hz limits are chosen to ensure that the sea clutter spectral density is below the noise density outside this frequency domain.

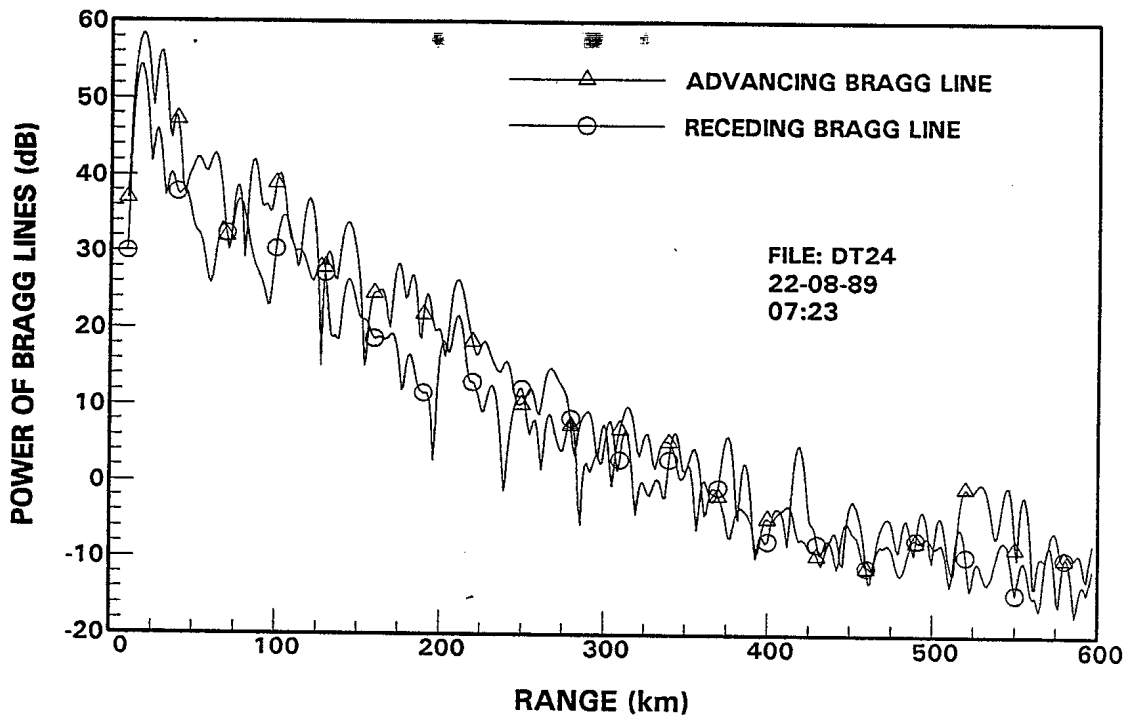


Figure 15. Spectral power of the Bragg lines as a function of range.

Figure 16 shows the spectral power of the sea-clutter continuum as a function of range. It shows generally a decreasing trend with respect to range. However, anomalous responses are observed in the range around 100 km and around 200 km. The increase in clutter power at these two ranges is attributed to the interference from sky wave propagation, probably from the E-layer of the ionosphere.

The sky wave interference appears to be time varying. Figure 17a shows the first 5120 samples of the I-channel time series extracted from range sample No. 95 of data file DT20. Since this range is in the neighborhood of 100 km, it exhibits the sky wave interference characteristics. Nevertheless, some characteristics of the Bragg lines can still be observed. Figure 17b shows the last 5120 samples of the same time series. The magnitude increased and the rate of fluctuation in the amplitude became more rapid. Figure 18a and 18b show the spectra calculated from the time series segments that correspond to those in Figures 17a and 17b, respectively. It can be seen that towards the end of the time series, the sea-clutter continuum has spread out in Doppler extent, and there are two spectral lobes centered about  $\pm 1$  Hz.

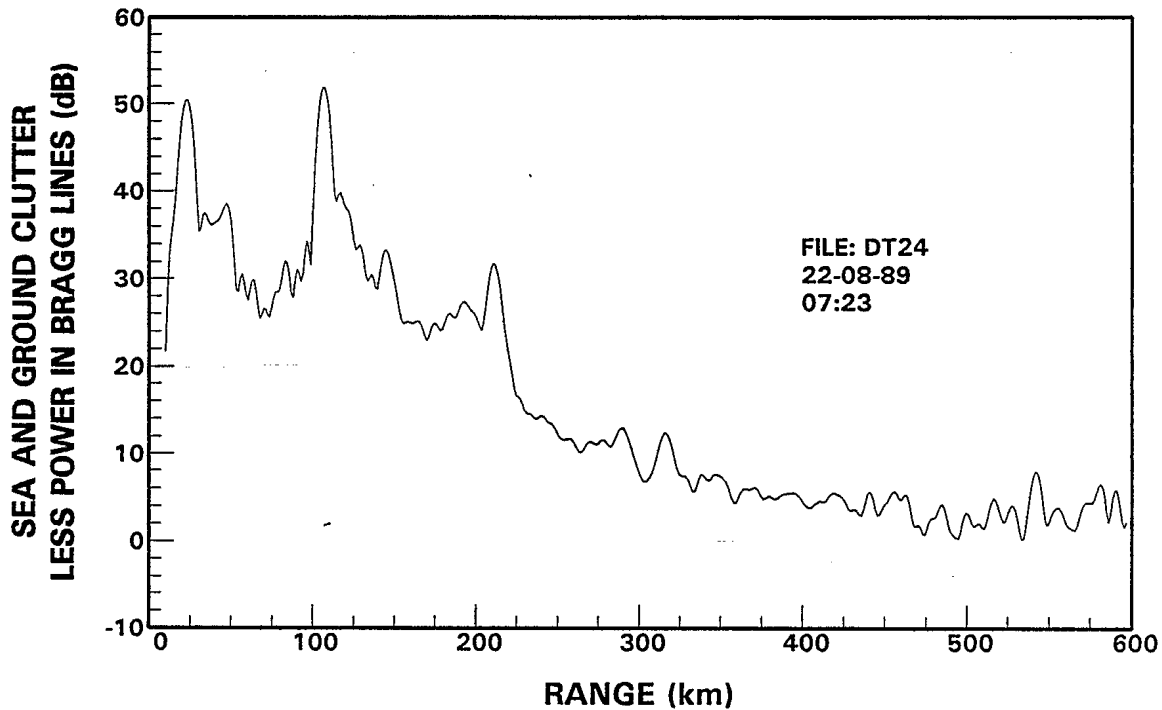


Figure 16. Spectral power of ground and sea clutter less power in Bragg lines.

#### 4.3.3 Noise density

The noise density can be estimated by summing the periodogram over a spectral region in which the sea-clutter spectral density is negligible. Normally this region will be between  $-12.5$  Hz and  $-1$  Hz and between  $1$  Hz and  $12.5$  Hz. However, since the periodogram contains spectral replica of the sea clutter at  $\pm 5$  Hz and  $\pm 10$  Hz, the spectral region around these frequencies cannot be used.

The noise density is approximated by summing the periodogram between regions  $(-4$  Hz,  $-1$  Hz) and  $(1$  Hz,  $4$  Hz) and then divide by the number of samples included in the two spectral regions. The unit of the noise density is dB/ $\Delta$  Hz, where  $\Delta = 25/N$  with  $N$  being the size of the periodogram.

Figure 19 shows the estimated noise spectral density as a function of range.

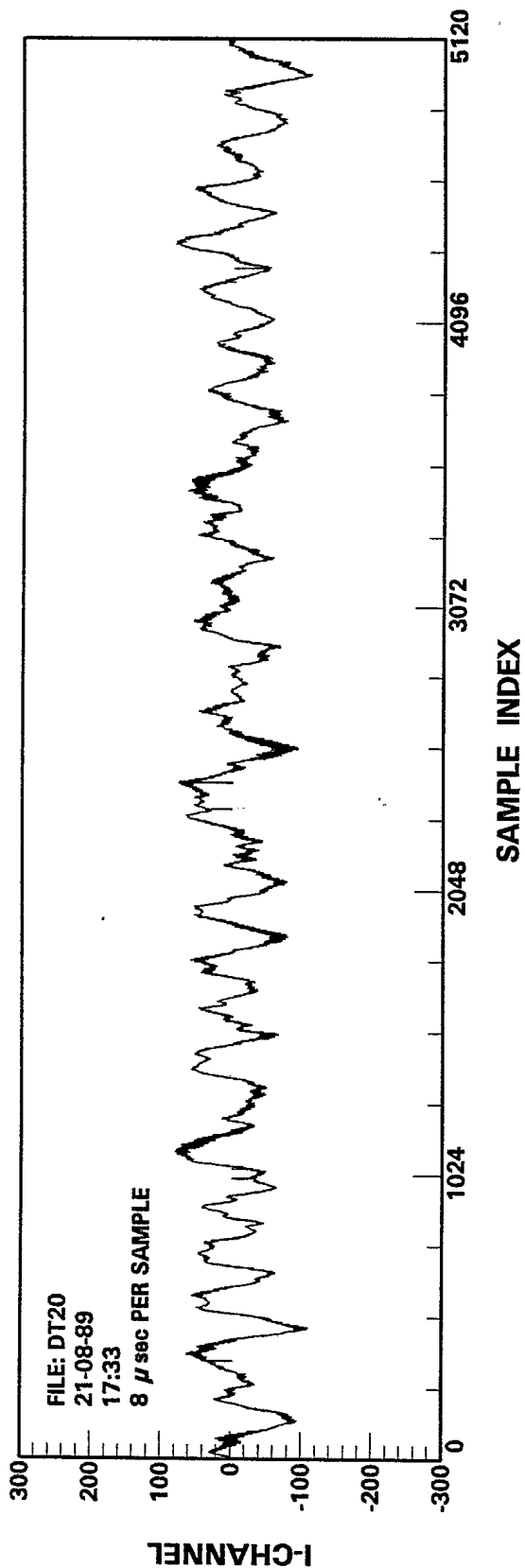


Figure 17a. I-channel waveform of an HFSWR time series during a period of moderate sky-wave interference.

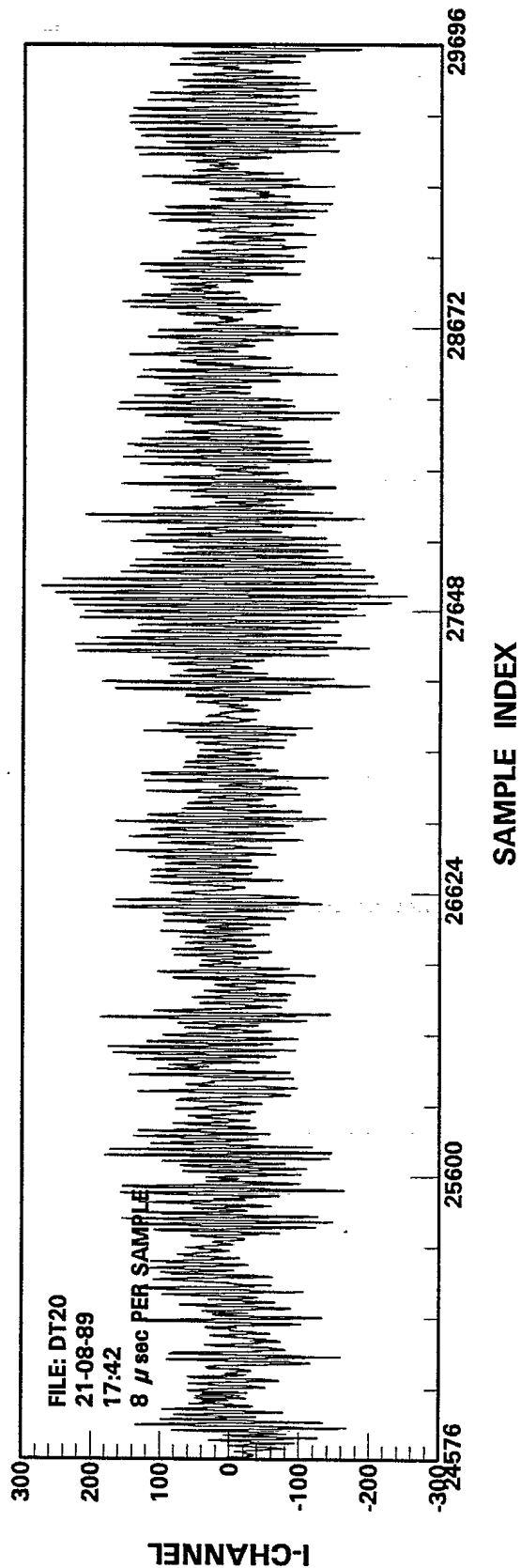


Figure 17b. I-channel waveform of an HFSWR time series during a period of severe sky-wave interference.

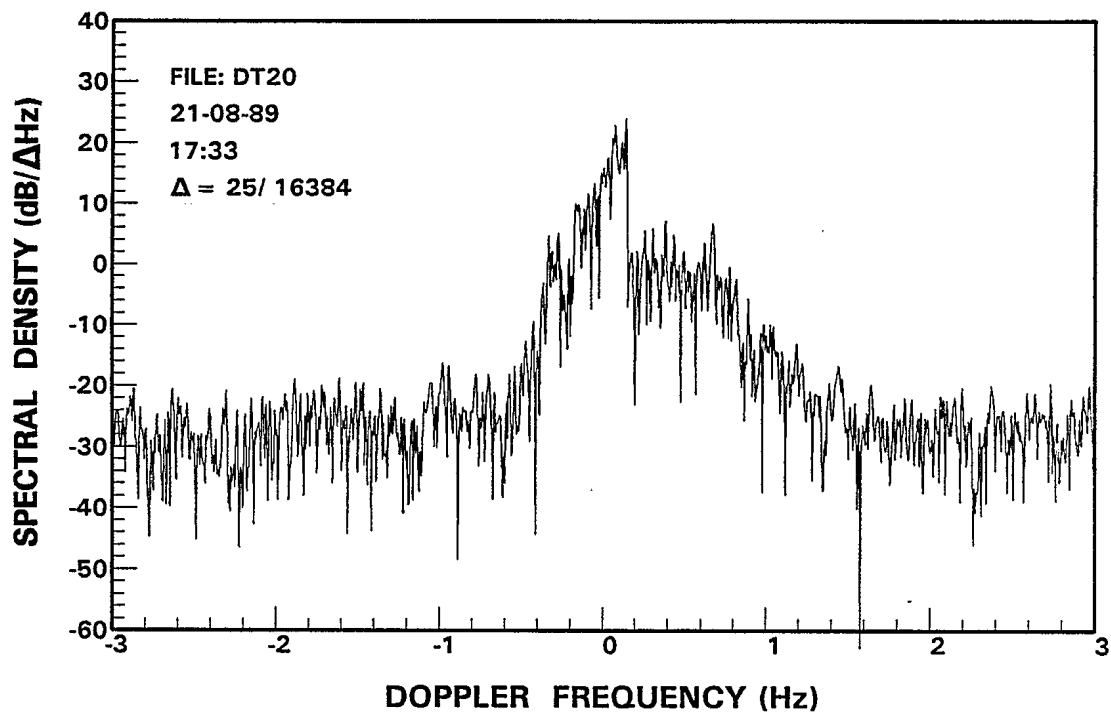


Figure 18a. Spectrum of the HFSWR time series of Figure 17a.

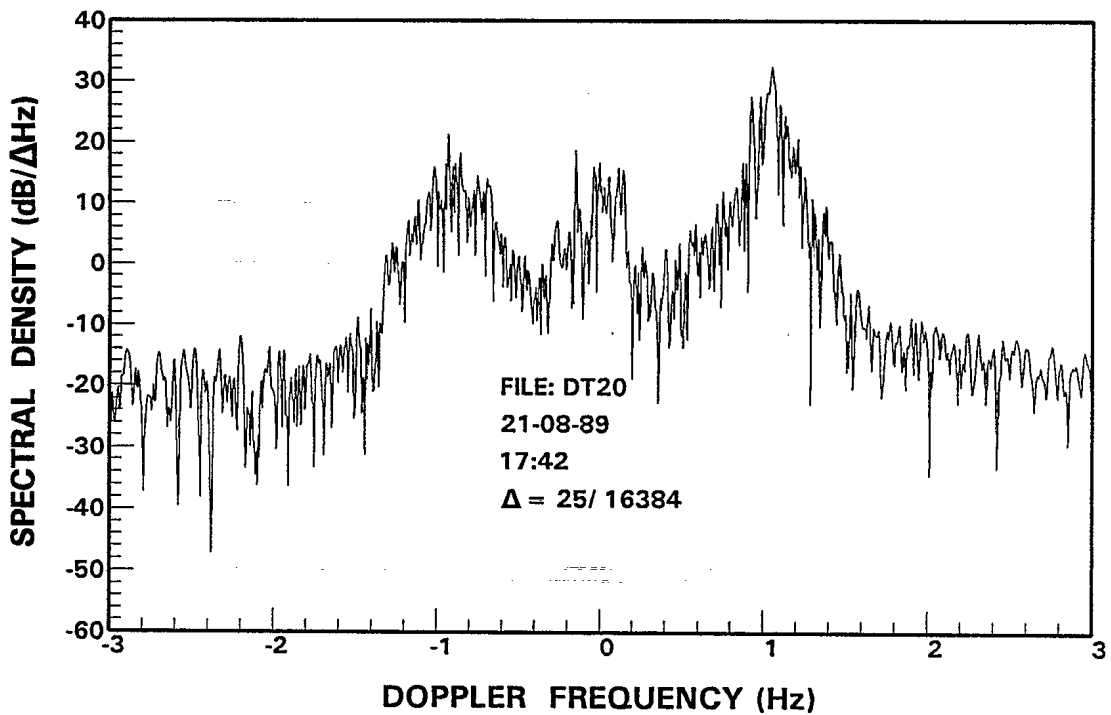


Figure 18b. Spectrum of the HFSWR time series of Figure 17b.

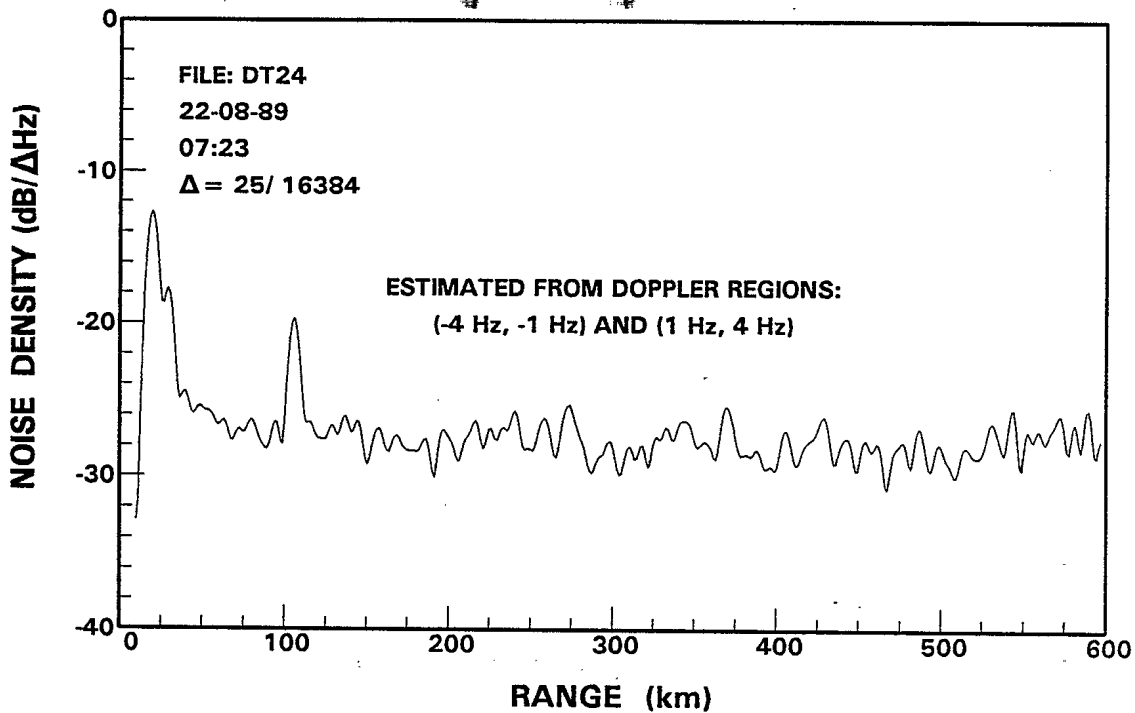


Figure 19. Noise density of HFSWR signal as a function of range.

It can be seen that the noise density is more or less independent of range as expected. The increased values of the noise spectral density observed at the 85th range sample (100 km) is attributed to sky wave interference. The large values observed at close-in ranges are attributed to the transient effect of the filters. It can be seen that, for range samples beyond 32, the noise spectral density is fairly close to the nominally constant value.

Hence in practice, we could consider that the transient effect of the FIR filters to be negligible after about 2/3 of the registers are filled with valid data. The rationale for this consideration is as follows.

FIR filters have tapped delay line architectures made up of shift registers. The data samples being filtered propagate from one shift register to the next every sampling interval. Strictly, for a FIR filter to attain its designed filtering characteristics, the registers must be filled with valid data.

Consider a 160-stage FIR filter to be used to filter the data contained in one of our HFSWR files. Since the 6th value in each data record is the first valid sample, this value will be the first sample to enter the FIR filter. We shall designate this data sequence as  $\{x_n, n=6,7,8,\dots,512\}$ . The valid filter output for a given input sample (e.g.,  $x_{32}$ ) is one taken at a time instant when that particular input sample has propagated to the center of the tapped delay line, or in the 80th shift register (to account for the group delay of the FIR filter), as illustrated in Figure 20. At the time the output sample  $y_{32}$  (for  $x_{32}$ ) appears, the first sample  $x_6$  is in the 107th shift register. This means that 107 out of 160, or about 2/3, of the shift registers are filled with valid data samples.

It is worth noting that the noise density does not increase appreciably for range samples beyond No.432 (512-80) which are also subjected to the transient effect of the FIR filter. This could mean that the rise in the noise density at close-in ranges is due to transient effect of the FIR filter in response to sea clutter which has a much larger magnitude than noise.

#### 4.4 Detection of ship and aircraft targets.

##### 4.4.1 Ship detection.

Most of the data files contain data from trial runs that involved the CFAV Bluethroat. The Bluethroat is a research vessel with a displacement of about 800 tons, which provided a large radar cross section. During the trial runs, the Bluethroat steamed towards or away from the radar at speeds up to 5 m/sec. Initial spectral analysis of selected data files showed that the detection of this vessel is feasible.

As an example, consider the experiment that commenced at 0730 on 22 August 1989. According to the data log, the Bluethroat began to steam towards the radar at a speed of 5.3 m/sec, with an initial range of 85 km. Thus one would expect to observe a strong Doppler component at 0.0689 Hz at the 62nd range sample. Figure 21 shows the spectrum of the time series of range sample No. 62. It can be seen that there is indeed a strong Doppler component at 0.0687 Hz.

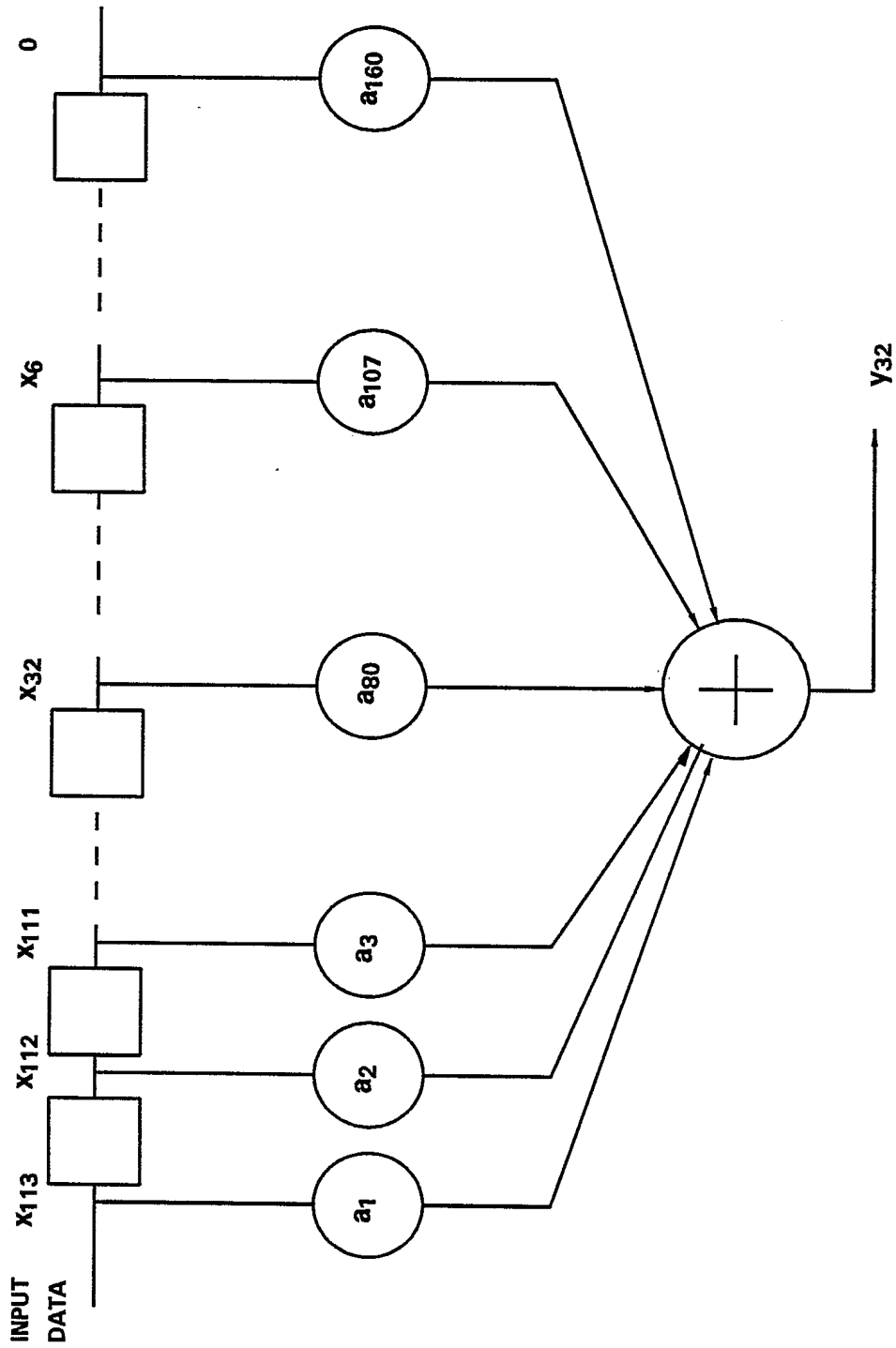


FIGURE 20. Data requirement for negligible transient effects from the 160-stage FIR filter.

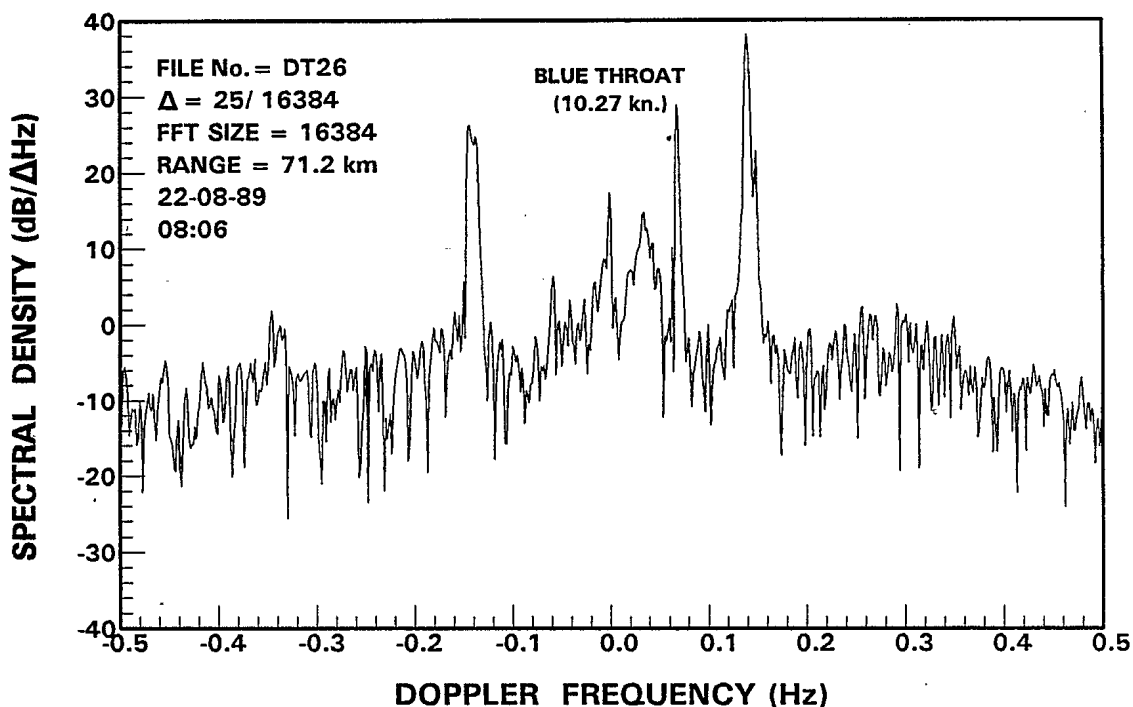


Figure 21. Spectrum of a HFSWR time series containing echoes from the CFAV Bluethroat.

The probability of detection cannot be meaningfully estimated until the probability densities of the sea clutter can be determined. The determination of the probability density function of the sea clutter will be a major topic of investigation in subsequent analysis of these data.

#### 4.4.2 Aircraft detection

Detection of relatively large aircraft is also shown to be feasible. A number of files contains data obtained from experiments that involved an Aurora aircraft. However, because of instrumentation problems, data are available with the aircraft at moderate ranges only (less than 65km or 35 n.m.). File DT15 is one such data set. Since an aircraft travels at speeds much higher than those of ships, the time duration in which the aircraft will stay in a single range gate is relatively short (less than 100 sec.). As a result, the coherent integration time used for aircraft target detection will necessarily be shorter than that for ship targets.

Figure 22 shows the periodogram computed from a 1024-point time series taken from the following experiment: File No. DT15, Range sample 9, starting time = 170 seconds after start. It can be seen that there exists a strong Doppler component at  $-2.0$  Hz which corresponds to a velocity of  $-153.85$  m/sec. The corresponding range of this range sample is 19.6 km. This agrees with the data log that the Aurora was traveling away from the radar at 300 knots. The target to noise ratio is about 25 dB. Hence the probability of detection for this target should be very high. It should be noted that this range sample is one of those that are affected by the transient response of the FIR filter. Hence one would expect to pick up a few more dB in target-to-noise-ratio at ranges beyond the 32nd range sample.

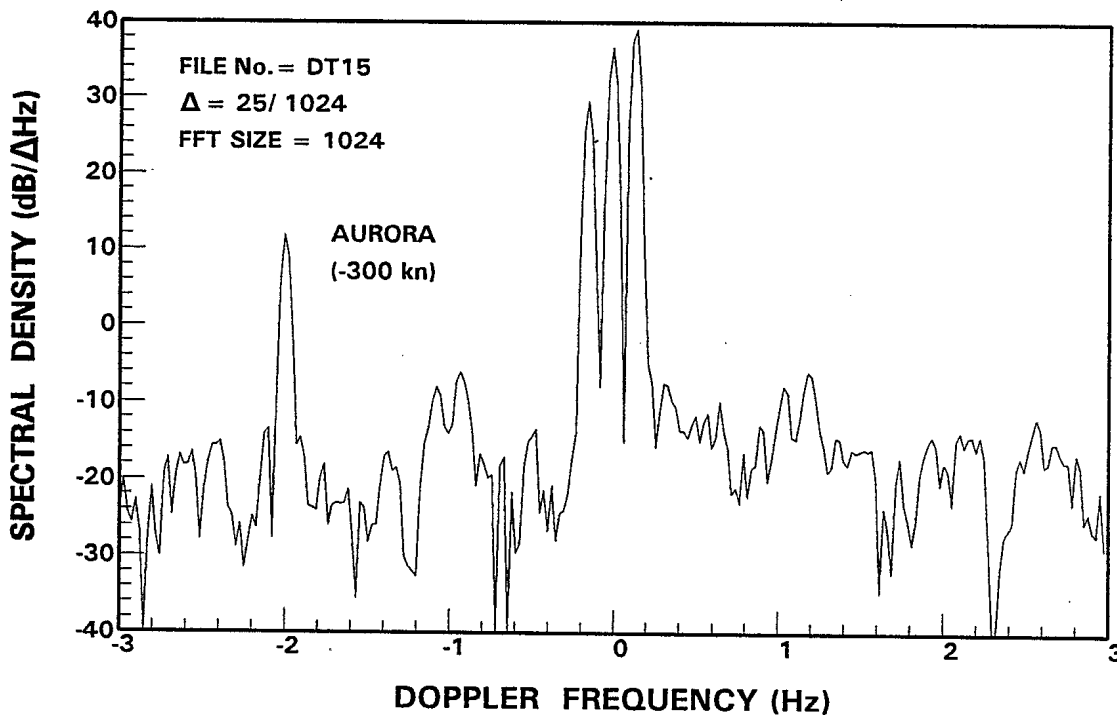


Figure 22. Spectrum of a HFSWR time series containing echoes from an AURORA aircraft.

## 5. Conclusion

### 5.1 Summary

Tapes containing raw data collected by NORDCO Limited in a HFSWR project are acquired by the Radar Division. Software for the conversion of these raw data into complex baseband time series is implemented on the Division's VAX computer and the Floating Point System array processor. Several deficiencies are observed in the data, including 60 Hz power source harmonic interferences and discontinuities in data sequence. The 60 Hz power source harmonics replicate the sea-clutter spectrum at 5 Hz intervals. As a result, high speed targets with a Doppler frequency near these values will be obscured. Means to suppress 60 Hz power source harmonic interference in the radar signal is explored. Results of preliminary analysis of some of the data show that conventional Doppler processing of the data permits the detection of ship and large aircraft targets.

It is also shown that HFSWR returns from certain range gates are subjected to interference from sky wave returns. This interference is observed to be time varying with periods of strong interference and fading lasting hundreds of seconds. These problems should be the subjects of future experimental investigation into HFSWR.

### 5.2 Plans for further analysis.

#### (a) Noise statistics

To evaluate the detection performance of the HFSWR for aircraft on a quantitative basis, the detection must be evaluated with the criteria of probability of detection at prescribed probability of false alarm. This requires the knowledge of the probability density of the noise. Some work has been reported in the literature [9] regarding HF noise statistics. However, it is important to compare results of experimental observation with those reported by other researchers.

The present set of data, containing 60 Hz harmonic interference, cannot be used directly to yield information on noise statistics. It may be possible to obtain valid results if the harmonic interference can be suppressed adequately. The interference suppression

technique outlined in Section 4.1 will be applied on these data to evaluate its effectiveness, and the result will be reported elsewhere [10].

(b) Sea-clutter statistics

The Doppler shifts of slow-moving targets such as surface vessels and icebergs fall in a region that is occupied by the sea clutter. The setting of the detection threshold for these target must take into account the sea clutter statistics. It is essential to gain some knowledge of the probability density function of the sea clutter, particularly in the regions around the two Bragg peaks.

(c) Time-domain behaviour of sea clutter

It was also observed that the magnitude of the sea clutter component from a fixed range cell varies with time. The variation of HF sea-clutter magnitude affects the setting of detection thresholds for ship targets. Consequently, it is important to gain some knowledge on the time domain behaviour of sea clutter. This knowledge could lead to predictive models that provide an estimate of the sea clutter amplitude from pulse to pulse, thereby permitting the suppression of sea clutter without adversely affecting the target signal.

(d) Target detection

It has been shown that the detection of ships and relatively large aircraft at long distance is possible using the HFSWR. However, no quantitative measure of the detection performance has been undertaken. To quantify the detection performance of HFSWR using measures such as probability of detection and probability of false alarm, accurate information on the probability densities of noise and sea clutter must be available.

There exist entries in the data log about a slower and smaller tracker aircraft. This aircraft has not been detected from the spectral analysis of the few data files examined thus far. We shall examine all available data carefully to determine the feasibility of using HFSWR to detect small aircraft targets such as the tracker aircraft. It is hoped that future experimental trials will furnish the required data to permit the determination of the capabilities and limitations of HFSWR.

## 6. References

- [1] A.M. Ponsford and S.K. Srivastava, "Ground wave radar development at NORDCO Limited – Phase 1, Part 1.", NORDCO Contract Report, 1990.
- [2] L.R. Rabiner and B. Gold, "Theory and application of digital signal processing", Prentice–Hall, Inc., Englewood Cliffs, N.J., 1975, pp. 194–204.
- [3] "FPS–5000 AP math library manual, Vol. 1–4", Floating Point System, Inc., No. 860–7437–011D, 1985.
- [4] "FPS–5000 Vector Function Chainer Manual – D.4", Floating Point System, Inc., No. 860–7437–020A, 1985.
- [5] P.E. Gill, W. Murray and M.H. Wright, "Practical optimization", Academic Press, New York, 1981.
- [6] F.J. Harris, "On the use of windows for harmonic analysis with the discrete Fourier transform", Proceedings of the IEEE, Vol.66, No.1, January 1978. pp. 51–83.
- [7] P.D. Welch, "The use of fast Fourier transform for the estimation of power spectra: A method based on time averaging over short, modified periodograms," IEEE Trans. on audio and electroacoustics, vol. AU–15, June 1967, pp.70–73.
- [8] S.K. Srivastava, "Scattering of high–frequency electromagnetic waves from an ocean surface: an alternative approach incorporating a dipole source", Ph.D. Thesis, Memorial University of Newfoundland, St. John's, Newfoundland, Canada, 1984.
- [9] D.E. Barrick, "The statistics of HF sea–echo Doppler spectra", IEEE Trans. on antenna and propagation, vol. AP–25, No.1, January 1977, pp. 19–28.
- [10] H. Leong, "Suppression of power line harmonic interference in HF Surface Wave Radar", DREO Report No. 1137, Defence Research Establishment Ottawa, Ottawa, Ontario, Canada, December 1992.

7. Acknowledgement

The author thanks Drs. T.N.R. Coyne and A.M. Ponsford for useful discussions and advices.

8. Appendix A: FORTRAN and AP FORTRAN source codes for HFSWR data pre-processing.

\*\*\*\*\* PROGRAM GFILE.FOR \*\*\*\*\*

PROGRAM GFILE

C  
C PURPOSE : TRANSFERS NORDCO RAW DATA FROM EXABYTE TO VAX DISK  
C FILES.  
C

```

CHARACTER*40 NAME
CHARACTER IOP,ASC(80)
INCLUDE '$(IODEF)'
INCLUDE '$(SSDEF)'
INTEGER*2 IBUF(8192),IOSB(4),MTP
INTEGER*4 MTD,SYSS$ASSIGN,SYSS$QIOW
EQUIVALENCE (ASC(1),IBUF(1))
TYPE 5
5 FORMAT('$ SPECIFY EXABYTE UNIT (0, 1) = ')
ACCEPT*,NT
IF(NT.EQ.0) ISTAT=SYSS$ASSIGN('MUB0',MTD,,)
IF(NT.EQ.1) ISTAT=SYSS$ASSIGN('MUB1',MTD,,)
IF(.NOT.ISTAT)CALL LIB$STOP(%VAL(ISTAT))
25 TYPE 30
30 FORMAT(' OPTION = (0) - REWIND; (1) - SKIP FILES;'/
1 10X,'(2) - BACK FILES; (3) - CREATE DISK FILE;'/
2 10X,'(>3) - EXIT; CHOICE = ')
ACCEPT*,JOP
IF(JOP.EQ.0)THEN
ISTAT=SYSS$QIOW(,%VAL(MTD),%VAL(IOS$_REWIND),IOSB,,
1 %VAL(1),,,,,,)
GO TO 25
ENDIF
IF(JOP.EQ.1)THEN
TYPE 40
40 FORMAT('$ SKIP FILES, HOW MANY? = ')
ACCEPT*,NFL
45 ISTAT=SYSS$QIOW(,%VAL(MTD),%VAL(IOS$_SKIPFILE),IOSB,,
1 %VAL(NFL),,,,,,)
GO TO 25
ENDIF

```

GFILE.FOR (Cont'd)

```

IF(JOP.EQ.2)THEN
TYPE 55
55  FORMAT('$ BACK FILES, HOW MANY? ')
ACCEPT*,NFL
  ISTAT=SYSSQIOW(,%VAL(MTD),%VAL(IOS_SKIPFILE),IOSB,,
1    %VAL(-NFL),,,,,,)
  ISTAT=SYSSQIOW(,%VAL(MTD),%VAL(IOS_SKIPRECORD),IOSB,,
1    %VAL(1),,,,,,)
GO TO 25
ENDIF
IF(JOP.EQ.3)THEN
TYPE 56
56  FORMAT('$ FILE NAME = ')
ACCEPT '(A)',NAME
OPEN(UNIT=1,FILE=NAME,ACCESS='SEQUENTIAL',
1   FORM='UNFORMATTED',STATUS='NEW')
ICOUNT=0
57  ISTAT=SYSSQIOW(,%VAL(MTD),%VAL(IOS_READLBLK),IOSB,,IBUF
1    ,%VAL(8192),,,,,)
ICOUNT=ICOUNT+1
TYPE*,ICOUNT,IOSB(1),IOSB(2),IOSB(3),IOSB(4)
IF(.NOT.ISTAT)CALL LIB$STOP(%VAL(ISTAT))
IF(1024.EQ.2160)THEN !CHECK FOR END OF FILE MARK.
GO TO 25
ENDIF
NWORD=IOSB(2)/2
DO J=1,NWORD
C
C   INTERCHANGE UPPER AND LOWER 8 BITS
C
  IBUF(J)=IISHFTC(1,IBUF(J),8,16)
ENDDO
WRITE(1)(IBUF(J),J=1,NWORD) !WRITE RECORD TO DISK FILE
GO TO 57
ENDIF
200 STOP
END

```

\*\*\*\*\* PROGRAM GENIQ\_LP\_AP.FOR \*\*\*\*\*

PROGRAM GENIQ\_LP\_AP

C  
C PURPOSE: READ NORDCO RAW DATA; (1)-SUBTRACT DC BIAS; (2)-MIX  
C DATA WITH 25 KHz SAMPLES TO COMPLEX BASEBAND;  
C (3)-LP FILTER; AND OUTPUT RESULT TO DISK FILES.  
C

CHARACTER IOP  
CHARACTER\*80 NAME  
CHARACTER\*20 NAMO  
CHARACTER\*7 ASC  
CHARACTER\*3 NUM  
INTEGER\*2 IBUF(512),JBUF(2048,512)  
INTEGER\*4 BCOUNT  
REAL\*4 BUF(53000),COEFBP(320),COEFLP(160),COST(2050)  
REAL\*4 SINT(1025),BUFI(1024),BUFQ(1024),COSTAB(5)  
REAL\*4 SINTAB(5)  
EQUIVALENCE (COEFBP(161),COEFLP(1)),(COST(1026),SINT(1))  
DATA NORD/160/,MAXB/30/

C  
C DC=362. !ADC BIAS VALUE  
C ASC='DT04L' !TIME SERIES FILE DESIGNATION

C  
C FIRST USABLE RANGE SAMPLE AT POSITION 6 OF INPUT RECORD.  
C

IFIRST=6  
ISTART=6

C  
C GENERATE TIME SERIES FOR ALL 507 RANGE SAMPLES.  
C

NCELLS=507

C  
C INPUT DATA IN FILE DT04.DAT OF DISK6 DIRECTORY  
C

NAME='DISK6:DT04.DAT'  
IOFSET=ISTART-1  
IEND=512-IOFSET  
JEND=NCELLS+80  
LENH=IEND+NORD\*2  
LEN=LENH\*2  
PI2BY5=6.2831853/5.

C  
C GENERATE SINE AND COSINE TABLES FOR THE 25 kHz MIXER  
C

DO I=1,5  
THETA=PI2BY5\*FLOAT(I-1)  
COSTAB(I)=COS(THETA)  
SINTAB(I)=-SIN(THETA)  
ENDDO

GENIQ\_LP\_AP.FOR (Cont'd)

```

C
DO I=1,205 !205 SETS OF 5 VALUES NEEDED FOR 1024 SAMPLES.
  JOFSET=(I-1)*5
  DO J=1,5
    J1=J+JOFSET
    COST(J1)=COSTAB(J)
    SINT(J1)=SINTAB(J)
  ENDDO
ENDDO

C
C READ BAND-PASS AND LOW-PASS FIR FILTER COEFFICIENTS (FIRST
C HALF)
C
  NORDH=NORD/2
  OPEN(UNIT=3,FILE='DISK6:COEF_BP.DAT',ACCESS='SEQUENTIAL',
1  FORM='UNFORMATTED',STATUS='OLD')
  READ(3)(COEFBP(I),I=1,NORDH)
  CLOSE(UNIT=3)
  OPEN(UNIT=3,FILE='DISK6:COEF_LP.DAT',ACCESS='SEQUENTIAL',
1  FORM='UNFORMATTED',STATUS='OLD')
  READ(3)(COEFLP(I),I=1,NORDH)
  CLOSE(UNIT=3)

C
C RECREAT THE OTHER HALF OF THE FILTER COEFFICIENTS
C
  DO I=1,NORDH
    II=NORD-I+1
    COEFBP(II)=COEFBP(I)
    COEFLP(II)=COEFLP(I)
  ENDDO

C
C AP ADDRESSES
C
  IADBUF=0      !DATA ARRAY ADDRESS IN AP
  IADCOS=65536-2050
  IADSIN=IADCOS+1025
  IADBPF=IADCOS-NORD*2
  IADLPF=IADBPF+NORD
  IADBFI=IADBUF
  IADBFQ=IADBFI+LENH
  JCOUNT=0

C
C INITIALIZE AP PROCESSOR AND PUT CONSTANT DATA INTO AP.
C
  CALL APINIT(0,0,ISTAT)
  CALL APPUT(COST,IADCOS,2050,2)

```

GENIQ\_LP\_AP.FOR (Cont'd)

```

C
C COSINE AND SINE TABLES
C
    CALL APWD
    CALL APPUT(COEFBP,IADBPF,320,2)
C
C BP AND LP FILTER COEF.
C
    CALL APWD
C
    OPEN(UNIT=1,FILE=NAME,ACCESS='SEQUENTIAL',
1     FORM='UNFORMATTED',STATUS='OLD')
    IFLAG=0          !RESET EOF FLAG
C
C ZERO MASTER DATA ARRAY
C
    ISTART=79 !VALID OUTPUT BEGINS WHEN SAMPLE PROPAGATES TO
35 DO J=1,53000 !CENTER OF FIR FILTER.
    BUF(J)=0.
    ENDDO
C
    DO J=1,32
    JP=ISTART+(J-1)*LEN !OFFSET POINTER FOR START OF DATA
C
    READ(1,ERR=38,END=40)(IBUF(K),K=1,512)
C
C CONVERT DATA FROM INTEGER TO REAL, CHECK FOR BAD DATA AND PLACE
C IN THE REAL PART OF BASEBAND SIGNAL BUFFER, WITH 80 LEADING
C ZEROS
C
38 DO K=1,IEND
    K1=K+IOFSET !STARTING INDEX FOR FIRST CELL
    K2=K+JP !STARTING INDEX FOR STORAGE IN BUF(.)
    IF (IBUF(K1).GT.30000.OR.IBUF(K1).LT.-30000.OR.
        IBUF(1).EQ.1) THEN
        BUF(K2)=0.
    ELSE
        BUF(K2)=IBUF(K1)-DC
    ENDIF
    ENDDO
    ENDDO
    ENDDO          !32 INPUT RECORDS STORED
    CALL APPUT(BUF,IADBUF,53000,2) !PUT DATA IN AP PAGE I
    CALL APWD
    CALL APLP(IFIRST,NCELLS)
    CALL APWR
C
    IDX=JCOUNT*32
    CALL APGET(BUF,IADBUF,53000,2)
    CALL APWD          !READ 32 PROCESSED RECORDS

```

GENIQ\_LP\_AP.FOR (Cont'd)

```

DO J=1,32
  IDX=IDX+1
  IDI=(J-1)*LEN
  IDQ=IDI+LENH
  I2=IDX*2
  I1=I2-1
  DO K=1,NCELLS
    I3=IDI+K+KOFSET
    I4=IDQ+K+KOFSET
    JBUF(I1,K)=ININT(BUF(I3))
    JBUF(I2,K)=ININT(BUF(I4))
  ENDDO
ENDDO
!PAGE I OF AP DONE
JCOUNT=JCOUNT+1
IF(JCOUNT.LT.32)GO TO 35

```

```

C
C WRITE DATA TO DISK FILE WHEN JCOUNT=32
C

```

```

  JCOUNT=0
  GO TO 45
40 IFLAG=1

```

```

C
C WRITE 1024-SAMPLE SEGMENT OF THE MIXED AND FILTERED TIME SERIES
C TO INDIVIDUAL DISK FILES
C

```

```

  45 BCOUNT=BCOUNT+1
!INCREMENT DATA BLOCK COUNTER
C

```

```

C OPEN OUTPUT FILES; THE FIRST RANGE CELL CORRESPONDS TO THE C
6TH SAMPLE.
C

```

```

  KOFSET=IFIRST-6
  DO I=1,NCELLS
    NI=I+IOFSET+KOFSET
    ENCODE(3,'(I3)',NUM)NI
    IF(NUM(1:1).EQ.' ')NUM(1:1)='0'
    IF(NUM(2:2).EQ.' ')NUM(2:2)='0'
    NAMO='DISK6: '//ASC//NUM//'.DAT'
    IF(BCOUNT.EQ.1)THEN
      OPEN(UNIT=2,FILE=NAMO,ACCESS='DIRECT',MAXREC=30,
1 RECL=1024,FORM='UNFORMATTED',STATUS='NEW')
    ELSE
      OPEN(UNIT=2,FILE=NAMO,ACCESS='DIRECT',MAXREC=30,
1 RECL=1024,FORM='UNFORMATTED',STATUS='OLD')
    ENDIF
    WRITE(2'BCOUNT)(JBUF(J,I),J=1,2048)
  ENDDO

```

```

C
  IF(BCOUNT.LT.MAXB.AND.IFLAG.EQ.0)GO TO 35
50 CLOSE(UNIT=1)
  STOP
  END

```

\*\*\*\*\* AP FORTRAN: APLP.FOR \*\*\*\*\*

DEFINE APLP(IFIRST,NCELLS)

```
"
" PURPOSE:   PERFORM MIXING AND LOW-PASS FILTERING ON NORDCO
"           HFSWR DATA ON THE FPS-5000.
"
" DEFINE LOCAL VARIABLE USED IN AP
"
"           LOCAL IADBUF, IADBFI, IADBFQ, IADCOS, IADSIN, IADBPF, IADLPF
"           LOCAL NORD, LENH, LEN, KCOUNT, LCOUNT, MCOUNT, NCOUNT, JEND
"           LOCAL IADWK, IEND, KEND, IDX, IDXI, IDXQ, IDUM, IDUM1, IADI, IADQ
"           LOCAL IDIFF
"
" 160-STAGE FIR FILTERS
"
"           IDIFF=IFIRST-6
"           NORD=160
"           JEND=NCELLS+80
"
" 507 RANGE CELLS TO BE PROCESSED
"
"           IEND=507
"
" LENGTH PER DATA SEGMENT = 507+TWICE THE FILTER LENGTH
"
"           IDUM=NORD*2
"           LENH=IEND+IDUM
"           LEN=LENH*2
"           JEND=IEND+NORD
"           IADBUF=0
"           IADCOS=65536-2050
"           IADCOS=63486
"           IADSIN=IADCOS+1025
"           IADBPF=IADCOS-320
"           IADLPF=IADBPF+160
"           IADBFI=IADBUF
"           IADBFQ=IADBFI+LENH
"           IADWK=IADBPF-1024
"           MCOUNT=0
LPO2: IDUM=MCOUNT*LEN
"           IDUM1=IDUM-1
"           IDX=IADBFI+IDUM1
"           IADI=IDX+1
"           IADQ=IADI+LENH
"           CALL VMUL(IADI,1,IADSIN,1,IADQ,1,JEND)
"           CALL VMUL(IADI,1,IADCOS,1,IADI,1,JEND)
"           IDXI=IADBFI+IDUM1
"           IDXQ=IADBFQ+IDUM1
"           IDXI=IDXI+IDIFF
"           IDXQ=IDXQ+IDIFF
```

AP FORTRAN: APLP.FOR (Cont'd)

```
LCOUNT=0
LPO4:  IDXI=IDXI+1
      IDXQ=IDXQ+1
      CALL VMUL(IDXI,1,IADLPF,1,IADWK,1,NORD)
      CALL SVE(IADWK,1,IDXI,NORD)
      CALL VMUL(IDXQ,1,IADLPF,1,IADWK,1,NORD)
      CALL SVE(IADWK,1,IDXQ,NORD)
      LCOUNT=LCOUNT+1
      IF LCOUNT < JEND GOTO LPO4
"
"INCREMENT DATA SEGMENT COUNTER
"
      MCOUNT=MCOUNT+1
      IF MCOUNT < 32 GOTO LPO2
      END
```

Note: Compilation and link procedures for AP FORTRAN are contained in [3] and [4].

## DOCUMENT CONTROL DATA

(Security classification of title, body of abstract and indexing annotation must be entered when the overall document is classified)

1. ORIGINATOR (the name and address of the organization preparing the document. Organizations for whom the document was prepared, e.g. Establishment sponsoring a contractor's report, or tasking agency, are entered in section 8.) Defence Research Establishment Ottawa 3701 Carling Ave., Ottawa, Ontario, K1A 0Z4, Canada		2. SECURITY CLASSIFICATION (overall security classification of the document, including special warning terms if applicable)  UNCLASSIFIED	
3. TITLE (the complete document title as indicated on the title page. Its classification should be indicated by the appropriate abbreviation (S,C or U) in parentheses after the title.)  Software Development and Analysis for High Frequency Surface Wave Radar Data. (U)			
4. AUTHORS (Last name, first name, middle initial)  Chan, Hing C.			
5. DATE OF PUBLICATION (month and year of publication of document)  December 1992	6a. NO. OF PAGES (total containing information. Include Annexes, Appendices, etc.)  47	6b. NO. OF REFS (total cited in document)  10	
7. DESCRIPTIVE NOTES (the category of the document, e.g. technical report, technical note or memorandum. If appropriate, enter the type of report, e.g. interim, progress, summary, annual or final. Give the inclusive dates when a specific reporting period is covered.)  DREO Report			
8. SPONSORING ACTIVITY (the name of the department project office or laboratory sponsoring the research and development. Include the address.) Defence Research Establishment Ottawa, 3701 Carling Ave., Ottawa, Ontario K1A 0Z4			
9a. PROJECT OR GRANT NO. (if appropriate, the applicable research and development project or grant number under which the document was written. Please specify whether project or grant)  041LR	9b. CONTRACT NO. (if appropriate, the applicable number under which the document was written)		
10a. ORIGINATOR'S DOCUMENT NUMBER (the official document number by which the document is identified by the originating activity. This number must be unique to this document.)  DREO Report No. 1153	10b. OTHER DOCUMENT NOS. (Any other numbers which may be assigned this document either by the originator or by the sponsor)		
11. DOCUMENT AVAILABILITY (any limitations on further dissemination of the document, other than those imposed by security classification)  <input checked="" type="checkbox"/> Unlimited distribution <input type="checkbox"/> Distribution limited to defence departments and defence contractors; further distribution only as approved <input type="checkbox"/> Distribution limited to defence departments and Canadian defence contractors; further distribution only as approved <input type="checkbox"/> Distribution limited to government departments and agencies; further distribution only as approved <input type="checkbox"/> Distribution limited to defence departments; further distribution only as approved <input type="checkbox"/> Other (please specify):			
12. DOCUMENT ANNOUNCEMENT (any limitation to the bibliographic announcement of this document. This will normally correspond to the Document Availability (11). However, where further distribution (beyond the audience specified in 11) is possible, a wider announcement audience may be selected.)  UNLIMITED			

13. ABSTRACT ( a brief and factual summary of the document. It may also appear elsewhere in the body of the document itself. It is highly desirable that the abstract of classified documents be unclassified. Each paragraph of the abstract shall begin with an indication of the security classification of the information in the paragraph (unless the document itself is unclassified) represented as (S), (C), or (U). It is not necessary to include here abstracts in both official languages unless the text is bilingual).

50// Processing software for data collected in an experimental High Frequency Surface Wave Radar (HFSWR) project is implemented in the VAX-3800 computer and the FPS-5000 floating point array process. The software is used to process the data in-house so as to obtain insights in HFSWR sea clutter, noise and target characteristics. The data are examined to assess quality. Several deficiencies are observed in the data, including 60 Hz power source harmonic interferences and discontinuities in data sequences. Preliminary analysis of some of the data shows that conventional Doppler processing of the data permits the detection of ship and large aircraft targets at fairly long ranges. Plans for further analysis of these data are discussed. //

14. KEYWORDS, DESCRIPTORS or IDENTIFIERS (technically meaningful terms or short phrases that characterize a document and could be helpful in cataloguing the document. They should be selected so that no security classification is required. Identifiers, such as equipment model designation, trade name, military project code name, geographic location may also be included. If possible keywords should be selected from a published thesaurus. e.g. Thesaurus of Engineering and Scientific Terms (TEST) and that thesaurus-identified. If it is not possible to select indexing terms which are Unclassified, the classification of each should be indicated as with the title.)

HIGH FREQUENCY RADARS, SURFACE WAVE, HF RADARS, CLUTTER, DOPPLER, DETECTION, IONOSPHERE.

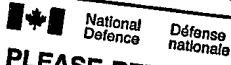
58  
10

H 128263

NO. OF COPIES NOMBRE DE COPIES	COPY NO. COPIE N°	INFORMATION SCIENTIST'S INITIALS INITIALES DE L'AGENT D'INFORMATION SCIENTIFIQUE
AQUISITION ROUTE FOURNI PAR	DAG	
DATE	DREO	
DSIS ACCESSION NO. NUMÉRO DSIS	04 March 1993	
93-00976		

DND T188 (6-87)

93-00976



**PLEASE RETURN THIS DOCUMENT  
TO THE FOLLOWING ADDRESS:**  
 DIRECTOR  
 SCIENTIFIC INFORMATION SERVICES  
 NATIONAL DEFENCE  
 HEADQUARTERS  
 OTTAWA, ONT. - CANADA K1A 0K2

**PRIÈRE DE RETOURNER CE DOCUMENT  
À L'ADRESSE SUIVANTE:**  
 DIRECTEUR  
 SERVICES D'INFORMATION SCIENTIFIQUES  
 QUARTIER GÉNÉRAL  
 DE LA DÉFENSE NATIONALE  
 OTTAWA, ONT. - CANADA K1A 0K2